

Urban water system theory and its model development and application

Jun XIA^{1,2}, Yongyong ZHANG^{1*}, Dunxian SHE², Shiyang ZHANG¹, Jun YANG³,
Mingquan LV⁴, Xiang ZHANG², Anqi LUO³, Shengjun WU⁴ & Yang LIU²

¹ Key Laboratory of Water Cycle and Related Land Surface Processes, Institute of Geographic Sciences and Natural Resources Research, Chinese Academy of Sciences, Beijing 100101, China;

² State Key Laboratory of Water Resources & Hydropower Engineering Sciences, Wuhan University, Wuhan 430072, China;

³ Aquatic EcoHealth Group, Key Laboratory of Urban Environment and Health, Institute of Urban Environment, Fujian Key Laboratory of Watershed Ecology, Chinese Academy of Sciences, Xiamen 361021, China;

⁴ Chongqing Institute of Green and Intelligent Technology, Chinese Academy of Sciences, Chongqing 400714, China

Received March 28, 2023; revised October 8, 2023; accepted November 8, 2023; published online January 31, 2024

Abstract The urban water system theory is an extension of the basin water system science on an urban scale, providing a new systematic solution for the unbalanced human-water relationship and severe water challenges, such as waterlogging, black and odorous water, and ecological degradation caused by urbanization. Most existing studies on urban water systems have focused on individual water cycle processes linked with water supply and sewage treatment plants, but mutual feedback between the water cycle and its associated material circulation and water ecology, as well as human processes, still needs further exploration. In this paper, the concept, theory, and technical methodology of the urban water system were developed based on the water cycle and basin water system science. The Urban Water System 5.0 (UWS 5.0) model was developed by integrating the Time Variant Gain rainfall-runoff Model with Urban water system (TVGM_Urban) in different underlying surface conditions for analyzing the natural-social water cycle processes and their associated water environmental and ecological processes and the influence of multiscale sponge measures. Herein, five major simulation functions were realized: rainfall-runoff-nonpoint source pollutant load, water and pollutant transportations through the drainage network system, terminal regulation and purification, socioeconomic water cycle, and water system assessment and regulation. The location for the case study used in this paper was Wuhan City. The findings showed that the entire urban water system should consider the built-up area and its associated rivers and lakes as the research object and explore the integrations among the urban natural-social water cycle and river regulations inside and outside of the city as well as the effects of socioeconomic development and sponge measures on the water quantity-quality-ecology processes. The UWS 5.0 model efficiently simulated the urban rainfall-runoff process, total nitrogen (TN) and total phosphorus (TP) concentrations in water bodies, and characteristic indicators of socioeconomic development. For the rainfall-runoff simulations, the correlation coefficient and Nash-Sutcliffe efficiency (NSE) fall under the excellent and good classes, respectively. For the TN and TP concentration simulations, results exhibited good bias and the correlation coefficients exceeded 0.90 for 78.1% of the sampled sites. The simulation of 18 socioeconomic indicators provided excellent bias, correlation coefficient, and NSE values of 100%, 83.3%, and 69.4% to total indicators, respectively. Based on the well-calibrated UWS 5.0 model, the source sponge, artificial enhancement, and source reduction-path interception-terminal treatment measures were optimized, which considerably mitigated waterlogging, black and odorous water, and lake eutrophication, respectively. The mitigation performance revealed that the maximum inundated area for a once-in-10-year rainfall event was reduced by 32.6%, the removal ratio of the black and odorous water area was 65%, the comprehensive trophic state index of water bodies was reduced by 37%, and the green development level of Wuhan City in 2020 increased from 0.56 to 0.67. This study is expected to advance the intersection and development of multidisciplinary fields (e.g., urban hydrology, environmental science, and ecology) and offer an important theoretical and technical basis for solving urban complex water issues and promoting green development of cities.

* Corresponding author (email: zhangyy003@igsnr.ac.cn)

Keywords Urban water system, Human-water relationship, Water issue, Green development, Theoretical basis, Mathematical model

Citation: Xia J, Zhang Y, She D, Zhang S, Yang J, Lv M, Zhang X, Luo A, Wu S, Liu Y. 2024. Urban water system theory and its model development and application. *Science China Earth Sciences*, 67(3): 704–724, <https://doi.org/10.1007/s11430-023-1226-9>

1. Introduction

The urban system is undergoing the highest intensities of socioeconomic activities and the most remarkable changes in the underlying surface, and it is also one of the regions with the most complex and easily unbalanced human-water relationship (Xia et al., 2017; Tian et al., 2018; Wang et al., 2021). Since the early 20th century, rapid urbanization in China has led to increasingly prominent water issues, including water security, water resources, and water environment and ecology, directly influencing urban green development (Liu et al., 2016). Examining and addressing the unbalanced human-water relationship is critical for solving the urban water issues comprehensively, and urgently needed for national policies on new urbanization construction.

Existing literature on the human-water relationship mainly focuses on the hydrologic cycle, water supply and drainage, biogeochemical cycle, pollutant transportation and transformation, water ecology, and response and carrying capacity of the water resource or ecological environment for human processes (e.g., urban expansion and economic development) (Xia et al., 2006; Fang et al., 2016; Wang et al., 2021). However, systematic research on the coupling mechanism of water-related processes (e.g., physical dynamic, biogeochemical, and human processes), human-water interaction, and its joint development along with complex underlying surfaces still needs support. With increasing global changes in research and advances in earth observation systems and high-performance computing, new hydrology disciplines have materialized, such as watershed system science and water system science (Cheng and Li, 2015; Jiang et al., 2020; Tang, 2020; Xia et al., 2021; Xia, 2023). Especially since the proposed Global Water System Project (GWSP) by the Earth System Science Partnership in 2004, the water cycle has been recognized as a crucial link between several water-related processes (GWSP, 2005; Sina and Anik, 2013; Bhaduri et al., 2014), which has greatly advanced the transformation of traditional monodisciplinary sciences (e.g., hydrology, environmental science, ecology, and water resource economics) into comprehensive water system science. Currently, water system science focuses on the mutual interaction among the water cycle and ecology, environment, energy, food, and human activities on a global or basin scale, coupled modeling and regulation, and so on, which provides a remarkable theoretical basis and new technical solution to solve water issues with regard to global change (Zhang et al., 2016b; Jiang et al., 2020). Nonetheless, the investigation and

regulation of the human-water relationship on an urban scale is still the forefront of the water system science (Xia et al., 2017).

This paper focuses on urban water issues and the human-water relationship and improves the concept, theory, and technical system of the urban water system based on the water system science and water cycle theory. In addition, the Urban Water System 5.0 (UWS 5.0) model is developed using the Urban Time Variant Gain rainfall-runoff Model (TVGM_Urban) as the core and integrating the natural-social water cycle and its associated water environmental, water ecological, and human processes with the model and effect of multiscale sponge measures. The theory and model are applied in Wuhan City. The study will promote the intersection and development of urban hydrology, environmental science, ecology, and other disciplines and offer a substantial theoretical and technical foundation for national policies on new urbanization construction.

2. Urban water system theory

2.1 Research progress on urban water system theory

An urban water system is the application and extension of basin water system science to the urban scale. It is a comprehensive system of multiple water cycle processes formed by the natural water cycle (e.g., precipitation, evapotranspiration, infiltration, runoff yield and routing, and regulation), socioeconomic water cycle (e.g., withdrawal, utilization, consumption, and discharge), and associated water environmental and ecological processes induced by nonpoint and point-source pollution (Figure 1a). Current studies on the urban water system have made significant progress in several aspects (Table 1). Particularly, due to the sponge city implementation in China, numerous studies and practices have shown that the solution to urban water issues requires comprehensive consideration of the interaction between the water cycle and its associated material cycles and water ecological processes. Thus, urban water system research has gradually shifted from traditional rainfall-runoff yield, water supply, and drainage processes to comprehensive multiple water system process research. Several theoretical works have emerged, such as Urban Water Cycle System 1.0–4.0 (Ren et al., 2012) and urban nature-society dualistic water cycle theory (Wang et al., 2021). Numerous application studies have primarily focused on urban planning and municipal construction, including gray infrastructure

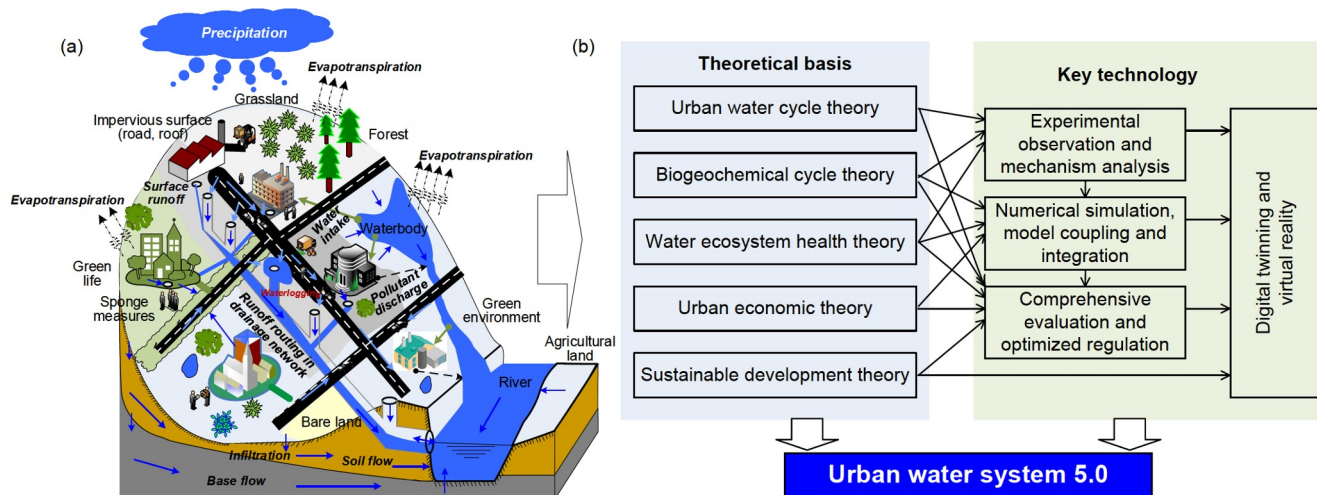


Figure 1 Urban water system (a) and its theoretical basis and key technologies (b).

construction, wastewater treatment, and sponge city construction (Zhang and Li, 2010). These achievements have significantly advanced the development and application of urban water system theory. However, further studies on integrated relationships among the water cycle, water environment, and ecology, linkages between the basin hydrological cycle and the urban drainage system, and regulation of socioeconomic development and sponge measures on multiple water cycle processes are still needed.

Xia et al. (2017) extended the concept of the urban water cycle system from the perspective of the natural water cycle, which emphasized the mechanism, system theory, and technological integration of the urban water cycles for different climatic zones and geographical subdivisions in China, that is, the UWS 5.0. In this version, the main research object was the built-up area and its associated rivers and lakes, while multiprocess integrations were explored, including “rainfall-evapotranspiration-storage-runoff” natural water cycle, “supply-use-consumption-discharge” artificial water cycle, river-city interaction, biogeochemical cycle, pollutant migration and transformation, and socioeconomic development using the hydrological cycle as a link and considering the multiple regulations of sponge measures on different scales (e.g., source low impact development (LID) measures on a patch scale, drainage areas on a medium scale, and rivers, lakes, and wetlands on a large scale), gray infrastructure for water supply and drainage (e.g., plants, networks, pumps, and gates), and rivers at the inside and outside the city. Moreover, earth system science and nonlinear time-varying system theories were adopted, and advanced technologies (e.g., *in-situ* or remote sensing monitoring, artificial intelligence, comprehensive evaluation, optimization and control, and digital twinning) were employed. This study, therefore, offers a new systematic solution for urban water management and green development.

2.2 Theoretical basis and key technologies of the urban water system

The theoretical bases for the urban water system (Figure 1b) mainly include the following:

(1) Urban water cycle theory. The water cycle theory represents the core of the urban water system theory. The urban water cycle is seriously affected by multiple factors, such as the expansion of impervious surfaces and drainage network systems, sponge-measure regulations, and climate change, causing synergistic changes in urban waterlogging, biogeochemical cycling, water quality, water ecosystem health, and socioeconomic development (Zhang et al., 2014; Zhang et al., 2019). Research on urban water systems is based on the water cycle theory and primarily investigates the effect of the precipitation and radiation changes due to urban construction and economic development on the water cycle processes (e.g., runoff generation, runoff routing, evapotranspiration, infiltration, and base flow). Additionally, the mutual interactions among the urban water system and climatological, environmental, ecological, and social systems are revealed (Xia et al., 2017).

(2) Biogeochemical cycle theory. The biogeochemical cycle theory mainly focuses on biogeochemical processes (e.g., absorption, decomposition, transformation, storage, release, and transport) of carbon, nitrogen, and phosphorus in the urban water cycle, ecological and socioeconomic systems, and the yield and discharge of different pollution sources, such as the accumulation-loss of nonpoint sources in complex underlying surfaces and collection-treatment-discharge processes of point sources related to the socioeconomic development (Chambers et al., 2016). Further, the theory reveals the driving mechanism of the material circulation on the spatiotemporal patterns of urban water quality, pollution, black and odorous water, and degradation of the

Table 1 Research progresses in the urban water system theory

| Research themes | Contents | References |
|---|---|--|
| Hydrological effects and waterlogging | Rainfall-runoff and runoff yield-routing mechanism, waterlogging, rain island and hydrological effects, sponge-measure regulation, rainwater and stormwater utilization, and so on | Smith et al., 2002; Shepherd, 2005; Amaguchi, 2012; Zhang et al., 2014; Liu et al., 2016; Zhang et al., 2018, 2022 |
| Water environmental effects and water pollution | Nonpoint source pollutant accumulation-flushing and loss, pollutant discharge and causes of water pollution due to socioeconomic development, water quality processes in drainage systems, and so on | Yang and Cheng, 2002; Ren et al., 2005; Obropta and Kardos, 2007; Freni et al., 2008; Sui et al., 2016; Zhou et al., 2022 |
| Water ecological effects and ecological degradation | Lake system evolution pattern, eutrophication and ecosystem health, ecological water demand, ecosystem services, and so on | Zhao and Yang, 2005; Zhang et al., 2007; Xu and Cao, 2009; Yu et al., 2011; Liang et al., 2016; Fu et al., 2017; Xu et al., 2020; Dou et al., 2022 |
| Socioeconomic development and carrying capacity of resource and environment | Water resources and urbanization, coordinated socioeconomic development, and water carrying capacity | Fang et al., 2004; Zuo et al., 2005; Xia et al., 2006; Yang et al., 2012 |
| Nature-society dualistic water cycle | Coupling of natural and social water cycles in urban areas, balance evolution, and so on | Wang et al., 2021 |
| Natural water cycle system (UWS1.0) | Green infrastructure self-purification processes, natural water supply and drainage processes, and so on | |
| Artificial water cycle systems (UWS2.0) | Gray infrastructure for water supply and drainage, artificial water cycle processes (tap water purification, sewage terminal treatment, and water supply and drainage) (i.e., “source-plant-network” system), and so on | Chen and Dong, 2007; Zhang and Li, 2010; Ren et al., 2012 |
| Combining gray and green and developing sponge measures for regulation (UWS3.0) | Gray-green integration. Focusing on the urban natural water cycle and sponge-measure regulation, artificial water cycle system, biogeochemical cycle and water quality processes, sewage terminal treatment and recycling processes, and so on | |
| Blue-green fusion and gray-green integration for urban water system theory (UWS4.0) | Blue-gray-green integration. Focusing on the urban natural water cycle and sponge measures regulation, artificial water recycling and excessive rainwater-runoff discharge system (i.e., “source-plant-network-river and lake”), biogeochemical cycle and water quality processes, sewage terminal treatment and recycling process, and so on | Ren et al., 2012 |
| Comprehensive development of the theoretical and technical systems for urban water systems (UWS5.0) | Taking the city and its associated rivers, lakes, and wetlands as the research object. Focusing on the integration of the natural water cycle (e.g., “rainfall-evapotranspiration-storage-runoff”), artificial water cycle (e.g., “supply-use-consumption-discharge”), and river regulation inside and outside the city, socioeconomic development, sponge-measure regulation and water quantity-quality-ecology processes, and so on | Xia et al., 2017; this study |

water ecosystem.

(3) Water ecosystem health theory. The water ecosystem in urban areas is formed as a result of the natural water ecosystem adapting to disturbances or reconstructions of urban residents and pollution discharge. It exhibits natural and artificial characteristics. The health of the urban water ecosystem focuses on its integrity, structure stability, urban water ecosystem function, and self-recovering ability after being subjected to disturbances (Karr et al., 1986; Shen et al., 2004). Particularly, it reveals the disturbance mechanism for human activities and hydrological, hydrodynamic, and water environmental changes on the water ecosystem and its self-recovering ability during urbanization.

(4) Urban economic theory. This theory mainly emphasizes the economic relations and laws existing in urban development, including urban expansion, population concentration and growth, industrial structure evolution and economic development, resource consumption, and pollution discharge (Balchin et al., 2000; Dong and Yang, 2021). Studies on urban socioeconomic development and its water cycle are based on the urban economic theory and examine the socioeconomic development laws, such as urban expansion and population concentration and evolution of the intake-use-consumption-discharge artificial water cycle. Results reveal the mutual interaction among the socioeconomics, water cycle, and ecological environment during

urbanization (Sivapalan et al., 2012; Fang et al., 2016; Lu et al., 2016; Tian et al., 2018).

(5) Sustainable development theory. This theory mainly focuses on the coordinated development of nature and society, and their fundamental relationships for resource utilization and guarantees fairness and consistency in resource allocation and utilization and the ecology, economy, and society sustainability (Zhang et al., 2007; Liu et al., 2018). Urban green development is based on the sustainable development theory, which estimates the carrying capacity and sustainability of urban water resources, ecology, and environment for socioeconomic development. Additionally, it explores the coordination between socioeconomic development and carrying capacity and develops various approaches for green development (Xia et al., 2006; Zou et al., 2022).

To support the practical applications of urban water system theory, the key technologies mainly include the following:

(1) Experimental observation and mechanism analysis. Long-term in-situ observation of representative regions (Zhang et al., 2019; Beal et al., 2020) or large-scale remote sensing hydrometeorological observation (Shepherd et al., 2002; Hu et al., 2018) is performed for obtaining a high-quality observation series (e.g., meteorology, hydrology, hydrochemistry, and pollutant concentration) under different underlying surfaces or sponge measures based on comprehensive management and application needs in urban water environment and ecology. Comparative analysis, regression analysis, or causal detection are adopted as the analytical techniques for urban hydrological and water environmental effects, revealing mechanisms such as urban runoff and pollution yield, water-heat balance and evaporation, and the underlying surface evolution and their regulations on the water cycle and water quality processes (Ren et al., 2005; Liu et al., 2014; Xu and Cheng, 2019; Chen et al., 2023).

(2) Numerical simulation and integration. The modeling techniques for various processes in the urban water system are improved based on experimental observations, mechanistic analysis, mass balance principles, and hydrodynamic and water quality models. For instance, the TVGM_Urban is utilized for developing the simulation module of rainfall-runoff-nonpoint source pollution load. The water flow of the drainage network system, water quantity and quality in the water body, and surface overflow are modeled using the hydrodynamic and water quality model or the water balance principle. Moreover, socioeconomic models and machine learning algorithms are used to simulate the socioeconomic water cycle (intake-use-consumption-discharge). Based on the above, the data transfer is solved through the sequential call of functional modules and resolution conversion of exchange variables on different temporal and spatial scales between the modules; furthermore, the uncertainty and calibration of the water system model are addressed via multi-objective optimization and error analysis (Zhang et al.,

2016a; Zhang and Shao, 2018).

(3) Comprehensive evaluation and optimized regulation. A comprehensive evaluation index system for green development is constructed in five dimensions, including resource utilization, environmental quality, ecological protection, economic growth, and green life, according to the requirements for the comprehensive green development evaluation of the urban water system, *Beautiful China Construction Assessment Indicator System and Implementation Plan* and inputs and outputs of the UWS 5.0 model. The comprehensive evaluation techniques for urban green development are developed by combining multiple-indicator weighting and evaluation methods (Xia et al., 2006; Zhang et al., 2007). Focusing on the nonlinear optimization and regulation problems of the urban water system, optimization regulation techniques are developed using the SCE-UA, genetic algorithm, particle swarm optimization, and NSGA-II multi-objective optimization algorithms and global or local optimizations are established as the objective functions for auto-optimizing the model inputs and parameters.

(4) Digital twinning and virtual reality. Three-dimensional (3D) simulation techniques of urban underlying surfaces and drainage network systems are developed through numerical simulations, 3D graphics, multimedia, and display and storage technologies to achieve systematic integration and visual display of the 3D models and multisource information databases for urban water systems (e.g., remote sensing and ground observation), model libraries (e.g., process, evaluation, control models), and result repositories (e.g., simulation and assessment results, control strategies). The spatial and temporal patterns of process simulations, comprehensive evaluation results, and their responses to different regulation strategies are emphasized (Gu et al., 2002; Bauer et al., 2021; Ye et al., 2022).

3. UWS 5.0 model

3.1 Model framework

The UWS 5.0 model is based on urban water system theory, takes TVGM_Urban as the core module, and extends the simulation modules of nonpoint source pollution, water, and pollutant transport in combined or diverted drainage network systems, waterlogging, socioeconomic water cycle, wastewater treatment, and water regulation and purification to realize the integrations of the natural-social water cycle, sponge-measure regulation (e.g., source LID, drainage areas, rivers, lakes, and reservoirs) on different scales, and water quantity-quality-ecological processes. There are five main simulation functions of UWS 5.0: Rainfall-runoff-nonpoint source pollutant load, water and pollutant transportations of the drainage network system, terminal regulation and purification, socioeconomic water cycle, water system assess-

ment and regulation (waterlogging simulation, black and odorous water assessment, ecological health assessment of lakes and reservoirs, and green development assessment and regulation). Figure 2 illustrates the model framework.

The rainfall-runoff-nonpoint source pollutant load module is designed based on the urban water cycle and biogeochemical cycle theories using the nonlinear time-variant runoff generation mechanism, pollutant accumulation and flushing mechanism, and water system simulation and integration techniques proposed by the author's research group. For analyzing the water and pollutant transportation, the drainage network system module, terminal regulation and purification module, and waterlogging simulation module are developed based on the mass and momentum conservation principle and obtained by solving Saint Venant equations. The socioeconomic water cycle module is developed based on the urban economic theory and machine learning algorithms or the Northam curve. The water system assessment and regulation module is primarily based on the water ecological health and sustainable development theories and achieves the integration, optimization, regulation, and visualization of the UWS 5.0 model via advanced techniques of numerical simulation and integration, comprehensive assessment, optimization and regulation, digital twinning, and virtual reality.

3.2 Rainfall-runoff-nonpoint source pollutant load module

3.2.1 Rainfall-runoff submodule

Using the nonlinear time-variant relationship between runoff generation, rainfall intensity, underlying surface type, and soil moisture proposed by Xia et al. (2005), the nonlinear TVGM_Urban model for complex urban land surfaces is derived and expressed as follows (Hu et al., 2021):

$$\begin{cases} G(t, i) = \alpha \cdot \{SW(t, i) / [W_{\text{sat}} \cdot SD \cdot C(i)]\}^{\beta} \cdot (I / I_m)^{\gamma}, \\ R(t, i) = \sum_{i=1}^N A(i) \cdot G(t, i) \cdot P(t) / At, \end{cases} \quad (1)$$

where $G(t, i)$ refers to the gain factor for the i th type of underlying surfaces at time step t ; R refers to surface runoff depth (mm); $SW(t, i)$ and W_{sat} refer to the soil moisture (mm) and saturated soil moisture capacity, respectively; SD refers to soil depth (mm); P refers to rainfall (mm); $C(i)$ refers to the influencing factor of the i th type of underlying surfaces; I and I_m refer to the current rainfall intensity and maximum rainfall intensity of the same month (mm min^{-1}), respectively; α , β , and γ refer to the model parameters; N refers to the total number of land cover types, where 10 land cover types are considered: road, roof, forest, grassland, water body, bare land, and sponge measures (e.g., sunken green space, pervious pavement, rain garden, and grassed swales). The overland flow routing submodule employs the overland flow routing equation proposed by Neitsch et al. (2011) to

measure the discharge from each land patch unit to the pipe node (inspection well or gutter inlet).

3.2.2 Nonpoint source pollution estimation submodule

This submodule considers the key processes of surface accumulation, atmospheric deposition, and flushing (e.g., dissolution and erosion) of multiple pollutants (e.g., sediment, chemical oxygen demand, nitrogen and phosphorus in various forms, heavy metals) for individual land cover types, where the accumulation of pollutants grows exponentially and converges to a certain threshold. The main equations for the i th land cover type and the j th nonpoint source pollutant are

$$\begin{cases} L(t, i, j) = B_{\text{max}}(i, j) \cdot [1 - e^{-K_B(i, j) \cdot t}] \\ \quad - WL(t, i, j) + S(t, i, j), \\ WL(t, i, j) = L(t, i, j) \cdot Rp(i, j), \end{cases} \quad (2)$$

where $L(t, i, j)$ refers to the surface pollutant accumulation rate per unit area ($\text{t km}^{-2} \text{yr}^{-1}$); $B_{\text{max}}(i, j)$ refers to the maximum surface pollutant accumulation rate per unit area ($\text{t km}^{-2} \text{yr}^{-1}$); $K_B(i, j)$ refers to a constant of the pollutant accumulation rate related to the anthropogenic activities in each land use type; $WL(t, i, j)$ refers to the pollutant export rate per unit area due to rainfall-runoff flushing ($\text{t km}^{-2} \text{yr}^{-1}$); $Rp(i, j)$ refers to the pollutant export coefficient; $S(t, i, j)$ refers to the pollutant atmospheric deposition rate per unit area ($\text{t km}^{-2} \text{yr}^{-1}$).

3.3 Water and pollutant transportation module of the drainage network system

3.3.1 Water and pollutant migration submodule of the drainage network system

For areas where detailed information on the drainage network system (e.g., pipe diameter, pipe length, burial depth, and flow direction) is available, the Saint Venant equations are solved for simulating the spatial variation in key hydrodynamic variables within the drainage network system, for example, flow velocity, discharge, and water depth. The water continuity and momentum equations in the drainage network system are expressed as follows:

$$\begin{cases} \frac{\partial Q_p}{\partial x} + \frac{\partial A_p}{\partial t} = \sum_{i=1}^N Q_{p, \text{up}}(i) + Q_{\text{sf}} + Wd, \\ \frac{\partial H_p}{\partial x} + \frac{v_p}{g} \cdot \frac{\partial v_p}{\partial x} + \frac{1}{g \cdot A_p} \cdot \frac{\partial Q_p}{\partial t} = S_0 - S_f, \end{cases} \quad (3)$$

where x refers to the distance (m); A_p refers to the wetted area (m^2); Q_p and v_p refer to the discharge ($\text{m}^3 \text{s}^{-1}$) and flow velocity (m s^{-1}) in the pipe, respectively; $Q_{p, \text{up}}(i)$ and Q_{sf} refer to the discharges in the i th pipe and from the surface to the pipe, respectively; N refers to the number of the upstream pipes connected to the pipe; H_p refers to the water depth (m); S_f and S_0 refer to the friction slope and bottom slope of the pipe,

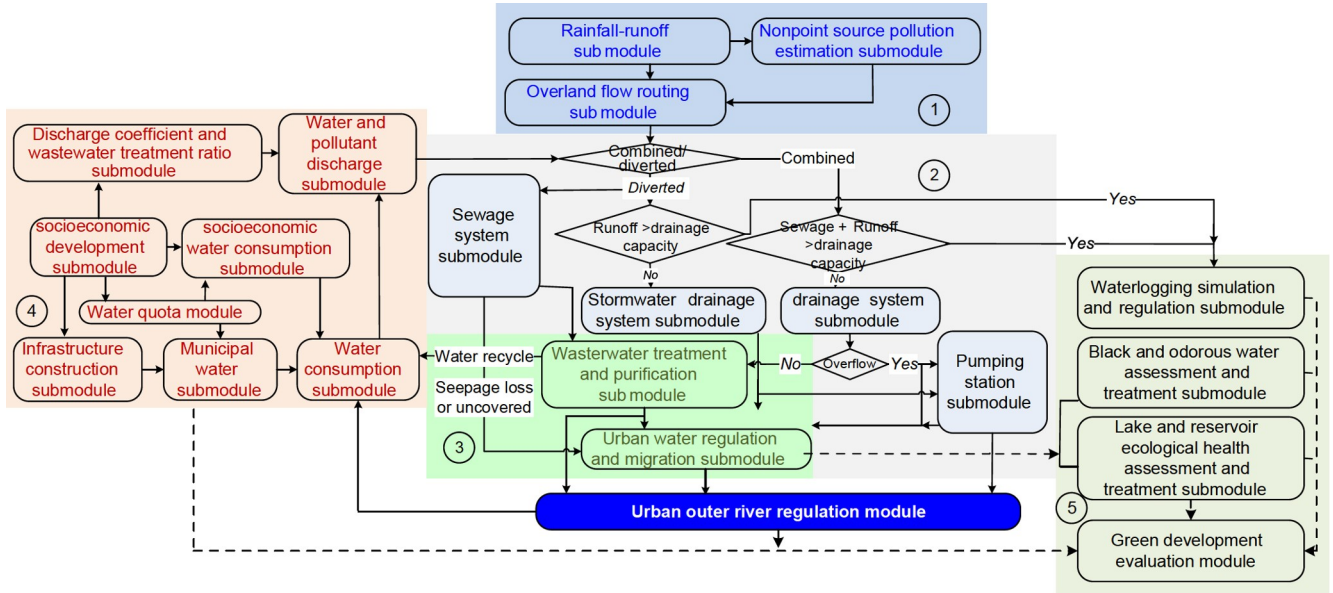


Figure 2 Framework of the UWS 5.0 model.

respectively; g refers to the gravitational acceleration; t refers to time (s); Wd refers to the point-source wastewater entering into the pipe ($\text{m}^3 \text{s}^{-1}$), including industrial and domestic sources. If the drainage network system is a combined system, the wastewater amount is estimated by the socioeconomic water cycle module; otherwise, if it is a diverted system, the wastewater amount in the stormwater drainage system is assumed to be zero, and all wastewater is discharged to the wastewater treatment plants via the sewage system.

The pollutant migration simulation is based on the mass balance principle, and mathematically,

$$\frac{dV \cdot C_p(j)}{dt} = \sum_{i=1}^N L_p(i, j) + WL(j) + Ld(j) - Q_p \cdot C_p(j) - K(j) \cdot V \cdot C_p(j) + S_p(j), \quad (4)$$

where V refers to the amount of water stored in the pipe (m^3); $C_p(j)$ refers to the j th pollutant concentration (mg L^{-1}); $L_p(i, j)$ and $WL(j)$ refer to the total load of the j th pollutant in the i th pipe and entering into the pipe from the land surface (g s^{-1}), respectively; $K(j)$ refers to the degradation coefficient of the j th pollutant; $S_p(j)$ refers to the source/sink term of the j th pollutant (g s^{-1}); $Ld(j)$ refers to the point-source pollution load entering into the pipe (g s^{-1}). The point-source load of the combined sewage system is estimated by the socioeconomic water cycle module, and that of the diverted sewage system is zero.

In areas where information on the drainage network system is not available, the drainage capacity of each pipe is estimated using the *Water Supply and Drainage Design Manual* (Chinese Edition). The drainage discharge rate, Q_p , and the overflow rate, $Q_{p,ov}$, of the pipe are measured by comparison of the receiving flow and the discharge capacity of the pipe (Zhang et al., 2018). Mathematically,

$$Q_{p,max} = 0.1 \cdot rc_d \cdot At \cdot c \cdot \frac{A_s + C_s \cdot 1gP_s}{(t + B_s)^{n_s}} + Wd, \\ Q_p = \begin{cases} \sum_{i=1}^N Q_{p,up}(i) + Q_{sf}, \\ \text{if } \sum_{i=1}^N Q_{p,up}(i) + Q_{sf} < Q_{p,max}, \\ Q_{p,max}, \\ \text{if } \sum_{i=1}^N Q_{p,up}(i) + Q_{sf} \geq Q_{p,max}, \end{cases} \quad (5) \\ Q_{p,ov} = \max\left(\sum_{i=1}^N Q_{p,up}(i) + Q_{sf} - Q_{p,max}, 0\right),$$

where $Q_{p,max}$ refers to the maximum discharge rate of the drainage network system ($\text{m}^3 \text{s}^{-1}$); At refers to the area of the drainage district (km^2); rc_d refers to the pipe coverage rate in the drainage district; t refers to the rainfall duration (min); c refers to the runoff yield coefficient; A_s , C_s , B_s , and n_s refer to the parameters related to the stormwater design formula; P_s refers to the return period of the drainage pipe (yr); Q_p and $Q_{p,ov}$ refer to the actual discharge rate and overflow rate ($\text{m}^3 \text{s}^{-1}$) of the drainage network system, respectively. Eq. (4) is also employed for simulating the pollutant migration process.

3.3.2 Outflow estimation submodule of the drainage network system

For the combined drainage network system, interception measures must be installed to prevent sewage discharging directly into urban water bodies. The outflow discharge on sunny days is the total amount of urban industrial wastewater and domestic sewage, and that on rainy days is the rainwater and sewage discharge. When the total outflow exceeds the

maximum interception flow, pipe overflow occurs, and vice versa, and the total outflow will be intercepted and migrated to the sewage treatment plants. The maximum intercepted flow can be computed with the flow multiplier method, interceptor design flow method, or spillway design method. The outflow discharge estimation equations are expressed as

$$\begin{cases} Q_{p,out} = \max(Q_p - Q_{int,max}, 0), \\ Q_{int,max} = \begin{cases} (n_0 - 1) \cdot Q_{sw}, \\ Q_{sewer}, \\ Q_{weir}, \end{cases} \\ Q_{p,int} = \begin{cases} Q_p & \text{if } Q_p < Q_{p,max}, \\ Q_{int,max} & \text{if } Q_p \geq Q_{p,max}, \end{cases} \end{cases} \quad (6)$$

where $Q_{int,max}$ refers to the maximum interception flow of the combined drainage network system ($m^3 s^{-1}$); n_0 refers to the interception multiplier; Q_{sewer} and Q_{weir} refer to the design flow rates of the interception pipe and the overflow weir ($m^3 s^{-1}$), respectively, which can be calculated using the upstream and downstream water levels of the facility and the corresponding hydrodynamic equations or specified by the user. The discharge of the pumping stations is primarily determined by the specific regulations.

3.4 Terminal regulation and purification module

3.4.1 Water quantity and quality regulation and migration submodule of the water body

For urban water bodies with detailed underwater topographic data, the submodule adopts the finite volume method to solve the two-dimensional unsteady shallow water equation to simulate the spatiotemporal changes of key variables such as flow field (x -direction flow velocity u and y -direction flow velocity v , $m s^{-1}$) and water depth (H_r , m) in urban water bodies. The hydrodynamic equations are as follows:

$$\begin{cases} \frac{\partial H_r}{\partial t} + \frac{\partial(H_r u)}{\partial x} + \frac{\partial(H_r v)}{\partial y} = \sum Q_{p,out} + Q_{os}, \\ \frac{\partial(H_r u)}{\partial t} + u \frac{\partial(H_r u)}{\partial x} + v \frac{\partial(H_r u)}{\partial y} = f H_r v \\ -g \frac{\partial H_r^2}{\partial x} - g H_r \frac{\partial z}{\partial x} - g n^2 u \frac{\sqrt{u^2 + v^2}}{H_r^{1/3}} \\ + \frac{\partial}{\partial x} \left(\varepsilon_x H_r \frac{\partial u}{\partial x} \right) + \frac{\partial}{\partial y} \left(\varepsilon_x H_r \frac{\partial u}{\partial y} \right) + \frac{C_a \rho_a W_x (W_x^2 + W_y^2)^{1/2}}{\rho}, \\ \frac{\partial(H_r v)}{\partial t} + u \frac{\partial(H_r v)}{\partial x} + v \frac{\partial(H_r v)}{\partial y} = -f H_r u \\ -g \frac{\partial H_r^2}{\partial y} - g H_r \frac{\partial z}{\partial y} - g n^2 v \frac{\sqrt{u^2 + v^2}}{H_r^{1/3}} \\ + \frac{\partial}{\partial x} \left(\varepsilon_y H_r \frac{\partial v}{\partial x} \right) + \frac{\partial}{\partial y} \left(\varepsilon_y H_r \frac{\partial v}{\partial y} \right) + \frac{C_a \rho_a W_y (W_x^2 + W_y^2)^{1/2}}{\rho}, \end{cases} \quad (7)$$

where x and y refer to the longitudinal and transverse flow

distances of water bodies (m), respectively; Q_{os} refers to the surface overland flow ($m^3 s^{-1}$); g means the gravitational acceleration; f refers to the Coriolis force constant (because the Coriolis force is the main force that acts on the flow of rivers and lakes, it is retained in the momentum equation); n refers to roughness; C_a refers to the wind resistance coefficient; ρ and ρ_a refer to water and air densities ($kg m^{-3}$), respectively; ε_x and ε_y refer to the eddy viscosity coefficients in the x - and y -directions ($m^2 s^{-1}$), respectively; W_x and W_y refer to the wind speeds in the x - and y -directions ($m s^{-1}$), respectively; t refers to time (s).

For urban water bodies with no underwater topographic data, the topological network of the flow direction is determined based on the numerical river network system, and the kinematic wave model or the Muskingum equations are employed for the simulation of the water regulation and transport processes. The spatial and temporal distributions of various pollutant concentrations (C_i) in the urban river network can be obtained using eq. (4).

3.4.2 Wastewater treatment and purification submodule

The submodule uses a black-box model for simulating the influence of different wastewater treatments on water quality concentration. Mathematically,

$$c_{out}(t, i) = k(i) \cdot c_{in}(t, i), \quad (8)$$

where $c_{out}(i)$ and $c_{in}(i)$ refer to the inflow and outflow concentrations of the i th pollutant in the sewage treatment facilities ($mg L^{-1}$), respectively; $k(i)$ refers to the removal rate of the i th pollutant, which is associated with the wastewater treatment; t refers to time (d).

3.5 Socioeconomic development and its water cycle module

3.5.1 Socioeconomic development submodule

This submodule simulates the interannual growth of the total population, urban population, urbanization rate, total urban gross domestic product (GDP), and secondary and tertiary industrial GDP and assumes that the total population growth rate is statistically related to the total population of the previous year or follows the Northam curve. The main equations are

$$\begin{cases} POP(t+1) = POP(t) \cdot [1 + R_{pop}(t)], \\ R_{pop}(t) = \begin{cases} a_{pop} \cdot POP(t-1)^2 + \\ b_{pop} \cdot POP(t-1) + c_{pop}, \\ a_{pop} / (1 + b_{pop} \cdot e^{-c_{pop}}), \end{cases} \\ UR(t) = a_{ur} / (1 + b_{ur} \cdot e^{-c_{ur}}), \\ POP_u(t) = POP(t) \cdot UR(t), \end{cases} \quad (9)$$

where POP and POP_u refer to the total population and urban

population (10^4); R_{pop} and UR refer to the annual population growth rate and urbanization rate, respectively; a_{pop} , b_{pop} , and c_{pop} refer to the parameters related to the annual population growth rate; a_{ur} , b_{ur} , and c_{ur} refer to the parameters associated with the urbanization rate; t refers to time (yr).

The GDP of the primary industry is assumed to be zero because of no agricultural activities in urban areas. The GDP growth of the secondary and tertiary industries assumes that the growth rate is statistically related to the population growth rate or follows the Northam curve. To estimate the GDP growth in urban areas,

$$\begin{cases} \text{GDP}_2(t+1) = \text{GDP}_2(t) \cdot [1 + R_{\text{GDP}_2}(t)], \\ \text{GDP}_3(t+1) = \text{GDP}_3(t) \cdot [1 + R_{\text{GDP}_3}(t)], \\ \text{GDP}(t) = \text{GDP}_2(t) + \text{GDP}_3(t), \\ R_{\text{GDP}_2}(t) = \begin{cases} a_2 \cdot R_{\text{POP}}(t)^2 + b_2 \cdot R_{\text{POP}}(t) + c_2, \\ a_2 / (1 + b_2 \cdot e^{-c_2 \cdot R_{\text{POP}}(t)}), \end{cases} \\ R_{\text{GDP}_3}(t) = \begin{cases} a_3 \cdot R_{\text{POP}}(t)^2 + b_3 \cdot R_{\text{POP}}(t) + c_3, \\ a_3 / (1 + b_3 \cdot e^{-c_3 \cdot R_{\text{POP}}(t)}), \end{cases} \end{cases} \quad (10)$$

where GDP, GDP_2 , and GDP_3 denote the total GDP in the urban area and the secondary and tertiary industrial GDP (10^8 yuan), respectively; R_{GDP_2} and R_{GDP_3} denote the annual growth rates of the secondary and tertiary industrial GDP, respectively; a_2 , b_2 , and c_2 refer to the parameters associated with the annual growth rate of the secondary industrial GDP; a_3 , b_3 , and c_3 denote the parameters associated with the annual growth rate of the tertiary industrial GDP; t means time (yr).

3.5.2 Infrastructure construction submodule

This submodule mainly simulates interannual changes in the investment of urban infrastructure development, drainage network system length, impervious surface, green space area, and so on. The model assumes a statistical relationship between the annual growth rate of the above indicators and the annual GDP growth rate or the investment in infrastructure construction. The investment equations are as follows:

$$\begin{cases} \text{Tinf}(t+1) = \text{Tinf}(t) \cdot [1 + R_{\text{inf}}(t)], \\ R_{\text{inf}}(t) = a_{\text{inf}} \cdot R_{\text{GDP}}(t)^2 + b_{\text{inf}} \cdot R_{\text{GDP}}(t) + c_{\text{inf}}, \end{cases} \quad (11)$$

where Tinf refers to the urban infrastructure construction investment (10^8 yuan); R_{inf} and R_{GDP} refer to the annual growth rates of the infrastructure construction investment and the total GDP, respectively; a_{inf} , b_{inf} , and c_{inf} refer to the parameters associated with the annual growth rate of infrastructure construction investment; t means time (yr).

The urban drainage pipe network system consists of stormwater, sewage, and combined pipes. To estimate their lengths,

$$\begin{cases} R_{\text{pcpd}}(t) = a_{\text{pcpd}} \cdot R_{\text{inf}}(t)^2 + b_{\text{pcpd}} \cdot R_{\text{inf}}(t) + c_{\text{pcpd}}, \\ L_{\text{pcpd}}(t+1) = L_{\text{pcpd}}(t) \cdot [1 + R_{\text{pcpd}}(t)], \\ R_{\text{wstd}}(t) = a_{\text{wstd}} \cdot R_{\text{inf}}(t)^2 + b_{\text{wstd}} \cdot R_{\text{inf}}(t) + c_{\text{wstd}}, \\ L_{\text{wstd}}(t+1) = L_{\text{wstd}}(t) \cdot [1 + R_{\text{wstd}}(t)], \\ rc_d(t+1) = rc_d(t) \cdot L_{\text{pcpd}}(t+1) / L_{\text{pcpd}}(t), \end{cases} \quad (12)$$

where L_{pcpd} and L_{wstd} refer to the lengths of the stormwater pipes or the combined pipes and the sewage pipes (km), respectively; R_{pcpd} and R_{wstd} refer to the annual growth rates of the stormwater pipes or the combined pipes and the sewage pipes, respectively; a_{pcpd} , b_{pcpd} , and c_{pcpd} refer to the parameters associated with the annual growth rates of the length of the stormwater pipes or the combined pipes; a_{wstd} , b_{wstd} , and c_{wstd} refer to parameters associated with the annual growth rate of the sewer pipe length; t refers to time (yr).

To estimate the urban impervious surfaces (e.g., roads and construction areas) and green areas,

$$\begin{cases} R_{\text{road}}(t) = a_{\text{road}} \cdot R_{\text{inf}}(t)^2 + b_{\text{road}} \cdot R_{\text{inf}}(t) + c_{\text{road}}, \\ A_{\text{road}}(t+1) = A_{\text{road}}(t) \cdot [1 + R_{\text{road}}(t)], \\ R_{\text{cons}}(t) = a_{\text{cons}} \cdot R_{\text{inf}}(t)^2 + b_{\text{cons}} \cdot R_{\text{inf}}(t) + c_{\text{cons}}, \\ A_{\text{cons}}(t+1) = A_{\text{cons}}(t) \cdot [1 + R_{\text{cons}}(t)], \\ R_{\text{green}}(t) = a_{\text{green}} \cdot R_{\text{inf}}(t)^2 + b_{\text{green}} \cdot R_{\text{inf}}(t) + c_{\text{green}}, \\ A_{\text{green}}(t+1) = A_{\text{green}}(t) \cdot [1 + R_{\text{green}}(t)], \end{cases} \quad (13)$$

where A_{road} , A_{cons} , and A_{green} refer to road, construction land, and green area (km^2), respectively; R_{road} , R_{cons} , and R_{green} refer to the annual growth rate of road, construction land, and green area, respectively; a_{road} , b_{road} , and c_{road} refer to the parameters associated with the annual growth rate of the road area; a_{cons} , b_{cons} , and c_{cons} refer to the parameters associated with the annual growth rate of the construction land area; a_{green} , b_{green} , and c_{green} refer to the parameters associated with the annual growth rate of the green land area; t refers to time (yr).

3.5.3 Socioeconomic water cycle submodule

The water use quota and discharge coefficient method are employed for estimating the interannual variability of the socioeconomic water withdrawal and pollution emission in a city. For estimating socioeconomic water withdrawals,

$$\begin{cases} Wu(t) = Wu_{\text{GDP}_2}(t) + Wu_{\text{POPu}}(t) + Wu_{\text{MW}}(t), \\ Wu_{\text{GDP}_2}(t) = RW_{\text{GDP}_2}(t) \cdot \text{GDP}_2(t), \\ Wu_{\text{POPu}}(t) = RW_{\text{POPu}}(t) \cdot \text{POP}_u(t), \\ Wu_{\text{MW}}(t) = [RW_{\text{green}} \cdot Fr_{\text{green}} \cdot A_{\text{green}}(t) \\ + RW_{\text{road}} \cdot Fr_{\text{road}} \cdot A_{\text{road}}(t)] / 10000, \end{cases} \quad (14)$$

where Wu refers to the total water consumption (10^4 m^3); Wu_{GDP_2} , Wu_{POPu} , and Wu_{MW} denote the industrial, domestic, and municipal water consumption, respectively (10^4 m^3);

RW_{GDP2} and RW_{POPu} refer to the per 10^4 yuan of GDP water consumption ($10^4 \text{ m}^3 \cdot 10^{-4} \text{ yuan}^{-1}$) and per capita comprehensive water consumption, respectively ($\text{m}^3 \text{ person}^{-1}$); RW_{green} and RW_{road} indicate the water quota for green space and road, respectively (L m^{-2}); Fr_{green} and Fr_{road} denote the green space and road watering frequency (yr^{-1}); t is time (yr). In general, recycled water is employed as municipal water, and the amount of socioeconomic water withdrawal is the sum of the industrial and domestic water use, $Wu_{GDP2} + Wu_{POPu}$.

RW_{GDP2} and RW_{POPu} are assumed to have power function relations with the secondary industrial GDP and total GDP, respectively, and their relations are as follows:

$$\begin{cases} RW_{GDP2}(t) = a_{RWGDP2} \cdot GDP_2(t)^{b_{RWGDP2}}, \\ RW_{POPu}(t) = a_{RWPOPu} \cdot GDP(t)^{b_{RWPOPu}}, \end{cases} \quad (15)$$

where a_{RWGDP2} and b_{RWGDP2} refer to the parameters associated with the water consumption amount per 10^4 yuan GDP; a_{RWPOPu} and b_{RWPOPu} refer to the parameters associated with the comprehensive water consumption amount per capita; t refers to time (yr). RW_{green} , RW_{road} , Fr_{green} , and Fr_{road} are calculated using the national water use standards, such as the *Standard for Comprehensive Water Consumption in Cities* (SL 367-2019) and *Design Code of Outdoor Water Supply* (GB 50013-2018).

To estimate the socioeconomic wastewater and pollution discharge,

$$\begin{cases} Wd(t) = Wu_{GDP2}(t) \cdot RD_{GDP2} \\ \quad + Wu_{POPu}(t) \cdot RD_{POPu}, \\ Ld(t, i) = \{ Wd(t) \cdot [1 - R_{sw}(t)] \cdot c_{out}(t, i) \\ \quad + Wd(t) \cdot R_{sw}(t) \cdot c_{in}(t, i) \} / 100, \\ R_{sw}(t) = a_{sw} \cdot R_{inf}(t)^2 + b_{sw} \cdot R_{inf}(t) + c_{sw}, \end{cases} \quad (16)$$

where Wd and Ld refer to the total urban drainage volume (10^4 m^3) and the total wastewater load (t), respectively; RD_{GDP2} and RD_{POPu} refer to the industrial and domestic wastewater discharge coefficients, respectively; R_{sw} refers to the urban wastewater treatment ratio, which is assumed to be causally related to R_{inf} ; a_{sw} , b_{sw} , and c_{sw} refer to the parameters related to the urban wastewater treatment ratio; i refers to the pollutant type; t refers to time (yr). Municipal water is involved in the urban natural water cycle, so it is not considered in this submodule.

3.6 Water system assessment and regulation module

3.6.1 Waterlogging simulation and regulation submodule

If the amount of water entering the drainage network system exceeds its drainage capacity, urban waterlogging is formed owing to the overflowing of the excess water from the drainage system to the land surface. This overflow rate

equals that of the drainage district $Q_{p,ov}$ in the waterlogging simulation module and can be computed with eq. (5). In addition, the inundation area and water depth are simulated by solving the two-dimensional unsteady shallow water equations using the finite volume method, which has the same principle as that of the water regulation and transport submodules, and the governing equations are still expressed with eq. (7) but by replacing $\sum Q_{p,out} + Q_{os}$ with $Q_{p,ov}$. The waterlogging control primarily adopts the sponge-measure regulation, drainage network system enhancement, terminal regulation, and so on. Waterlogging prevention and control are realized via the optimization of the land cover types and their areas in the rainfall-runoff submodule, pipe diameters and coverage ratio in the water and pollutant migration submodule of the drainage network system, and water area and depth in the water quantity and quality regulation and migration submodules of the water body.

3.6.2 Black and odorous water assessment and treatment submodule

The pollutant concentration (e.g., COD_{Cr} , NH_4^+-N , and TP) output from the water quantity and quality regulation and migration submodules of the water body are employed for evaluating the black and odorous levels (mild, moderate, or severe levels) in water. Moreover, 14 processes, including ecological restoration (i.e., submerged plants, floating plants, ecological floating islands, and emergent plants), active water circulation (i.e., fixed-pipeline and mobile-boat oxygenation), and artificial enhancement (i.e., artificial water plants and in-situ and bypass purification devices), are provided for treating the black and odorous water. Based on the black and odorous level, the submodule can recommend various process combinations, and their corresponding treatment effects and costs can be estimated. Key process parameters can also be optimized by the user, such as the removal efficiency, economic cost, and response time.

3.6.3 Lake and reservoir ecological health assessment and treatment submodule

The comprehensive nutrient status index is calculated using the comprehensive nutrient status index method, considering the water quality concentration, such as TN, TP, chlorophyll-a, and COD_{Mn} of the lakes and reservoirs, which are output from the water quantity and quality regulation and migration submodules of the water body. This strategy overcomes the limitations of single-indicator assessment. The equations are

$$\begin{cases} \text{CTLI} = \sum_{j=1}^m w(j) \cdot \text{TLI}(j), \\ w(j) = r_j^2 / \sum_{j=1}^m r_j^2, \end{cases} \quad (17)$$

where CTLI is the comprehensive nutrient status index; m is

the number of selected water quality indicators; $w(j)$ is the weighting coefficient for the j th water quality indicator with chlorophyll-a as a reference; r_j is the correlation coefficient between the j th water quality indicator and chlorophyll-a concentration; $TLI(j)$ is the nutrient status index for the j th water quality indicator. The equations can be found in Wang et al. (2002). In general, if $CTLI < 30$, it is oligotrophic; if $30 \leq CTLI \leq 50$, it is mesotrophic; if $50 < CTLI \leq 60$, it is mildly eutrophic; if $60 < CTLI \leq 70$, it is moderately eutrophic; if $CTLI > 70$, it is highly eutrophic. The submodule also provides a multilevel ecological restoration measure library for source control, pathway dissipation, and terminal treatment for ecological management of lakes and reservoirs, as well as the effectiveness, economic cost, and applicability of these measures. Based on the measure applicability, natural geography, and eutrophication level of rivers and lakes, feasible ecological restoration actions are recommended, and their effectiveness and cost are determined.

3.6.4 Green development evaluation submodule

Establishing an index system to assess green development is based on indicators presented in the Assessment Indicator System and Implementation Program for the Construction of a Beautiful China, the Opinions of the CPC Central Committee and the State Council on the Promotion of Ecological Civilization, and the Green Development Indicators developed by the National Development and Reform Commission (NDRC) and the input and output variables of the UWS 5.0 model. Eighteen relevant indicators are selected from five dimensions. These dimensions are as follows: (1) resource utilization: total water consumption (10^4 t), decrease rates of water consumption per 10^4 yuan GDP (%) and per unit of secondary industry GDP (%), and decrease rate of construction area per unit of GDP (%); (2) environmental quality: decrease rates of the total COD_{Cr} and NH_4^+-N emissions (%), centralized sewage treatment rate (%), number of black and odorous water bodies, and water quality standard-reaching ratio of the water function zone (%); (3) ecological protection: woodland coverage ratio (%), and eutrophication level in lakes and reservoirs; (4) economic growth: GDP per capita growth rate (%), per capita disposable income (yuan), and the ratio of tertiary industrial GDP to total GDP (%); (5) green life: decrease rate of domestic water consumption (%), urban green coverage ratio (%), waterlogging point numbers, and sewage network length (km). To eliminate the uncertainty of a single method for the evaluation results of green development, the model adopts the entropy-based TOPSIS model, comprehensive index method, comprehensive multiplier method, comprehensive weight method, and evaluation method proposed by NDRC for evaluating the green development level, and the median of the five evaluation results is considered the final result of the green development evaluation.

3.7 Module integration in the UWS 5.0 model

The UWS 5.0 model exhibits wide variability in the spatial and temporal scales of its modules and simulates numerous variables, making the module integration extremely challenging. The model uses the water cycle as the link and encapsulates all modules into five major functional modules based on the module function. Formatted text reading and writing are utilized for facilitating data transfer between different modules, thereby realizing module integration of the UWS 5.0 model. Figure 3 illustrates the integration framework.

The main coupling approach is as follows: The discharge (Q_{sf}) and water quality process (WL) entering into each node of the drainage network system are calculated using the rainfall-runoff and nonpoint source pollution load estimation submodules, which are then loaded into the water and pollutant transportation module of the drainage network system. The in-pipe migration and surface overflow of water quantity and quality variables (Q_p , H_p , C_p , $Q_{p,ov}$, and $C_{p,ov}$) are simulated with the water and pollutant migration submodule of the drainage network system, and its outflow estimation submodule is employed to calculate the water quantity and quality processes ($Q_{p,out}$ and $C_{p,out}$). The water quantity and quality regulation and migration submodule of the water body and the wastewater treatment and purification submodule are then driven to determine the water quantity and quality processes that are loaded to the urban outer river regulation module. Subsequently, the socioeconomic development and its water cycle module estimate the wastewater and pollution load (Wd and Ld), which are loaded into the water and pollutant transportation module of the drainage network system, water quantity and quality regulation and migration submodule of the water body, and wastewater treatment and purification submodule. The surface overflow process ($Q_{p,ov}$) acquired from the water and pollutant transportation module of the drainage network system is employed to drive the waterlogging simulation and regulation submodule. The pollutant concentration (C_r) process in urban water bodies acquired from the terminal regulation and purification module is utilized to drive the black and odorous water assessment and treatment as well as lake and reservoir ecological health assessment and treatment submodules, respectively. Based on this, the socioeconomic development and its water cycle module, waterlogging simulation and regulation submodule, black and odorous water assessment and treatment submodule, and lake and reservoir ecological health assessment and treatment submodule are employed for calculating the green development indicators and driving the green development evaluation submodule to achieve the green development evaluation of the city. The main modules of the UWS 5.0 model are programmed using Fortran, C, and other languages, and the model parameters are customized using the JSON data exchange format. At last, the sequential

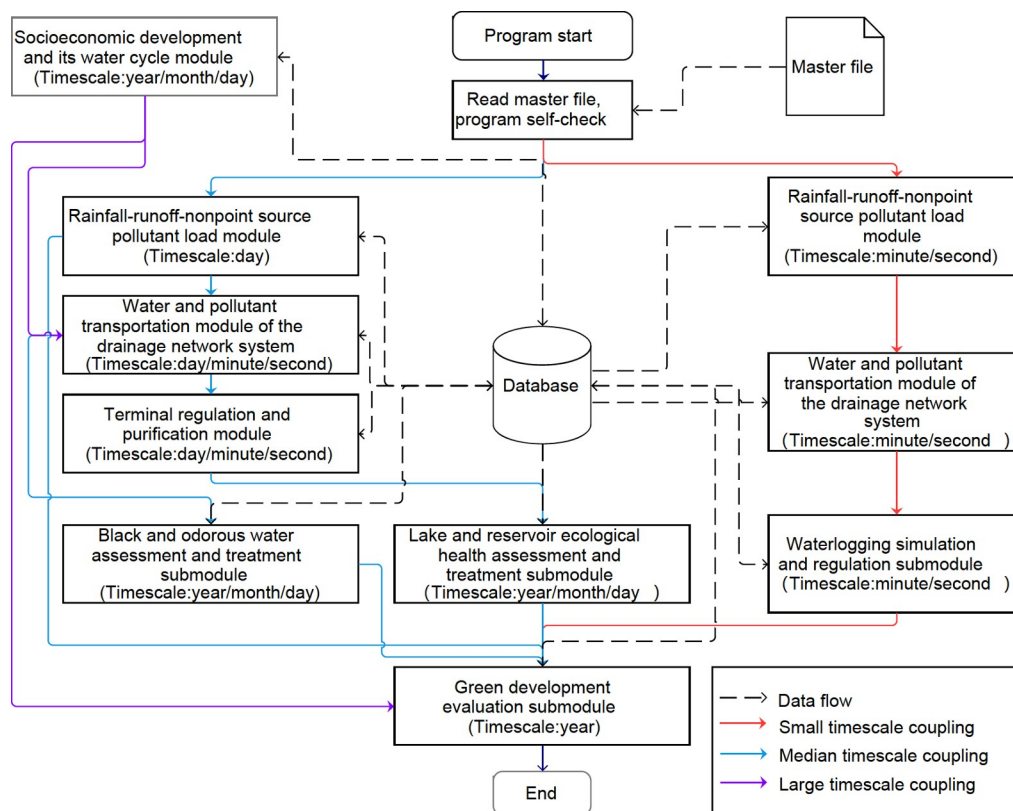


Figure 3 Module integration procedure of the UWS 5.0 model.

invocation of various modules and procedures is achieved using the BAT batch files.

3.8 Performance evaluation and parameter calibration

The UWS 5.0 model can simulate many urban hydrodynamics, water quantity and quality, and socioeconomic variables. For evaluation of the model performance, it is recommended to use bias, correlation coefficient (r), and NSE. The performance ratings are excellent, good, fair, and poor as per literature (Santhi et al., 2001; Moriasi et al., 2007; Ritter and Muñoz-Carpena, 2013; Zhang et al., 2016a) and given in Table 2. Due to the different computational times of the different modules, model calibration is conducted by combining automatic optimization and manual calibration. For instance, the hydrological, water quality, and socioeconomic parameters are calibrated by automatic optimization, while manual calibration is performed on the hydrodynamic parameters. The objective function is a weighted function of bias, r , and NSE (Zhang et al., 2022).

4. Application of a typical city in the Yangtze River Economic Belt

4.1 Overview of Wuhan City

Wuhan is one of China's 14 megacities, and its geographical

location and economic status play a crucial role in the Yangtze River basin. With accelerating urbanization, water issues such as urban flooding, water pollution, and ecological degradation, become more prominent and directly limit the green development of the city. Thus, this work examines the causes of water issues in Wuhan City and its management countermeasures from the perspective of the urban water system.

4.2 Data collection and model setup

The basic data sources mainly include geographic information, hydrometeorological, water quality monitoring, and socioeconomic data. The geographic information data include the digital elevation model (DEM: 30 m×30 m) acquired from the Resource and Environmental Science and Data Center of the Institute of Geographic Sciences and Natural Resources Research, Chinese Academy of Sciences (<https://www.resdc.cn/>), land use data (2 m×2 m) from Gaofen-1 remote sensing image interpretation, attribute data of the drainage network system (e.g., the pipe shape, pipe diameter, burial depth, direction, location, and depth of rainwater outlets), and water quality observations. The hydrometeorological data are the measured daily rainfall, maximum and minimum temperature data during 2001–2020 at eight stations in Wuhan City and its surroundings from the National Meteorological Data Network (<http://data.cma.cn/>),

Table 2 Criteria for the UWS 5.0 model performance evaluation

| Indicator | Statistic | Performance rating | | | |
|---------------|-----------|--------------------|--------------------------------|--------------------------------|---------------------------|
| | | Excellent | Good | Fair | Poor |
| Hydrodynamics | bias | [-0.05, 0.05] | (0.05, 0.20] or [-0.20, -0.05) | (0.20, 0.30] or [-0.30, -0.20) | (0.30, +∞) or (-∞, -0.30) |
| | <i>r</i> | [0.95, 1.00] | [0.85, 0.95) | [0.80, 0.85) | (-∞, 0.80) |
| | NSE | [0.90, 1.00] | [0.70, 0.90) | [0.65, 0.70) | (-∞, 0.65) |
| Hydrology | bias | [-0.05, 0.05] | (0.05, 0.20] or [-0.20, -0.05) | (0.20, 0.30] or [-0.30, -0.20) | (0.30, +∞) or (-∞, -0.30) |
| | <i>r</i> | [0.85, 1.00] | [0.75, 0.85) | [0.70, 0.75) | (-∞, 0.70) |
| | NSE | [0.75, 1.00] | [0.60, 0.75) | [0.50, 0.60) | (-∞, 0.50) |
| Water quality | bias | [-0.20, 0.20] | (0.20, 0.40] or [-0.40, 0.20) | (0.40, 0.70] or [-0.70, -0.40) | (0.70, +∞) or (-∞, -0.70) |
| | <i>r</i> | [0.80, 1.00] | [0.70, 0.80) | [0.65, 0.70) | (-∞, 0.65) |
| | NSE | [0.65, 1.00] | [0.50, 0.65) | [0.40, 0.50) | (-∞, 0.40) |
| Socioeconomic | bias | [-0.30, 0.30] | (0.30, 0.50] or [-0.50, 0.30) | (0.50, 0.75] or [-0.75, -0.50) | (0.75, +∞) or (-∞, -0.75) |
| | <i>r</i> | [0.80, 1.00] | [0.65, 0.80) | [0.55, 0.65) | (-∞, 0.55) |
| | NSE | [0.65, 1.00] | [0.40, 0.65) | [0.30, 0.40) | (-∞, 0.30) |

four measured rainfall events, and the associated outflow of the drainage network system in the Yingwuzhou community. The water quality monitoring data are sampling data collected from 16 sites in two field surveys in 2019 and 2020, including the TN and TP concentrations. The socioeconomic data are the Statistical Bulletin of Wuhan National Economic and Social Development 2001–2020 of the Wuhan Bureau of Statistics (<http://tjj.wuhan.gov.cn/>), which includes the total population, urbanization rate, secondary and tertiary industrial GDP, infrastructure investment, green area, sewage and drainage pipe length, the areas of roads and construction land, sewage treatment rate, industrial and domestic water consumption, water supply, water drainage, and so on. Based on the DEM, spatial road and community distribution, and drainage pipe and stream directions, the urban area of Wuhan is divided into 438 hydrological response units with 1,492 minimum computation units and the drainage network system is generalized into 642 pipes and 693 nodes, with a total length of 794.1 km (Figure 4). The waterlogging simulation and source regulation performance assessment take the Qingshan District Sponge City Demonstration Zone, namely, the PPP zone, as the study area, which is divided into about 224,000 grids with 5 m×5 m resolution. The lake hydrodynamics and water quality simulations take the water network of the Greater Donghu Lake, consisting of the Donghu, Yanxihu, Yandonghu, Shahu, and Beihu Lakes, as the study area, which is divided into 2,970, 1,324, 3,103, 3,212, and 1,748 grids with 100 m×100 m, 100 m×100 m, 50 m×50 m, 30 m×30 m, and 30 m×30 m, resolutions, respectively.

4.3 Model validation

The simulated hydrological, water quality, and socioeconomic development processes of the UWS 5.0 model for Wuhan City are validated with limited collected observations, including rainfall-runoff submodule, nonpoint source pollution load estimation submodule, water and pollutant transportation module of the drainage network system, water quantity and quality regulation and migration submodule of the water body, and socioeconomic development submodule, which basically cover the main modules of the UWS 5.0 model. Moreover, the reliability of the simulation results is further improved by comparison with the literature on Wuhan City.

Four measured runoff events in the Yingwuzhou community on 2005-06-10, 2005-06-26, 2005-07-10, and 2005-08-03 are employed for calibrating and validating rainfall-runoff submodule parameters. The first three events are utilized for calibration, while the last one is employed for validation (Figure 5). The findings reveal that the bias in 75% of events is within the fair limits (within ±0.30), and correlation coefficients and NSEs are in excellent (>0.85) and good (>0.60) classes for all events, respectively. Zhang et al. (2022) introduced in detail the calibration and validation procedures. Moreover, the simulated runoff coefficients for all hydrological response units are in the range of 0.51–0.61, consistent with runoff coefficients of 0.49–0.85 reported in the literature for Wuhan City (Liu, 2009; Chen, 2018).

For the nonpoint source pollution load estimation sub-

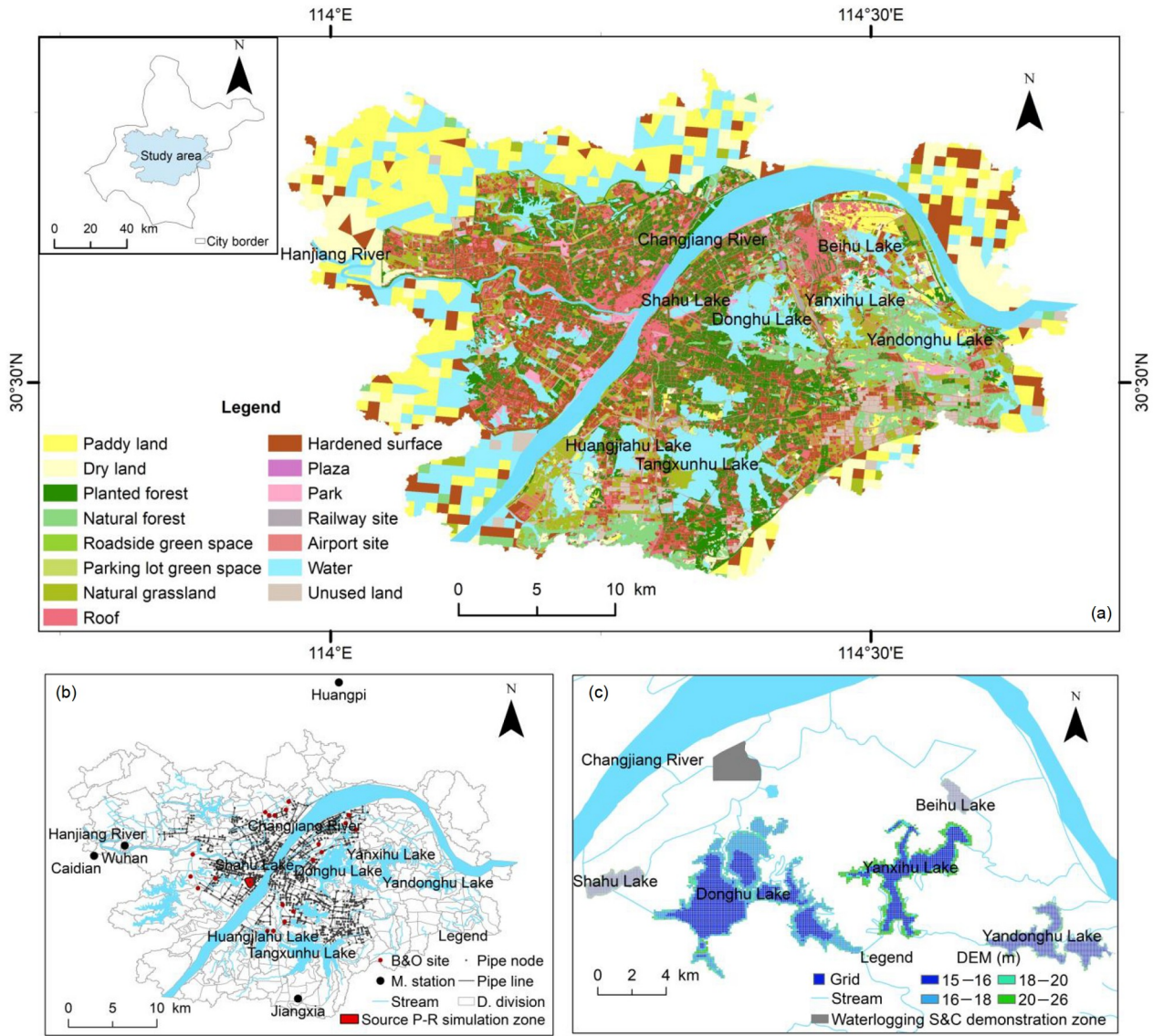


Figure 4 Model application area and land use (a), drainage subdivision and pipe network (b), and computational gridding of the major lakes (c). B&O site: black and odorous water monitoring site. M. station: meteorological station. D. division: drainage divisions. Source P-R simulation zone: source precipitation-runoff simulation zone. Waterlogging S&C demonstration zone: waterlogging simulation and control demonstration zone.

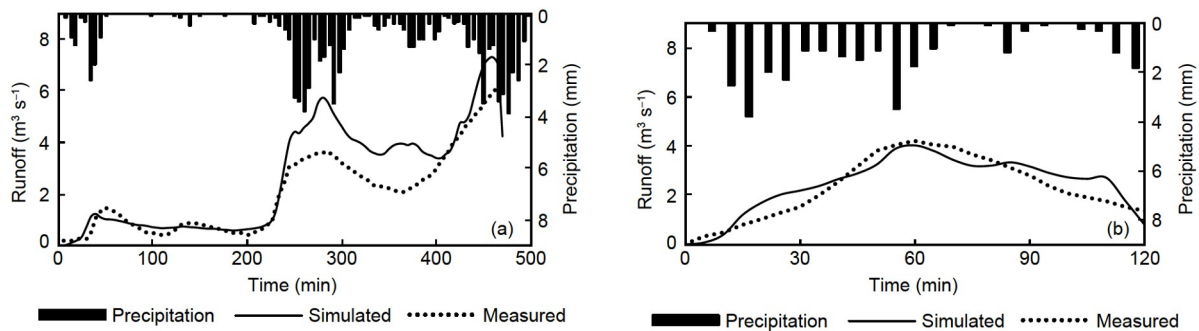


Figure 5 Comparison of the measured and simulated rainfall-runoff processes on 2005-06-26 (a) and 2005-08-03 (b) in the Yingwuzhou community.

module and water quantity and quality regulation and migration submodule of the water body, the measured pollutant concentration data from 16 water bodies for 2019 and 2020

are employed for calibrating and validating the submodules (Figure 6). In the calibration and validation periods, the correlation coefficients of TN concentration are 0.96 and

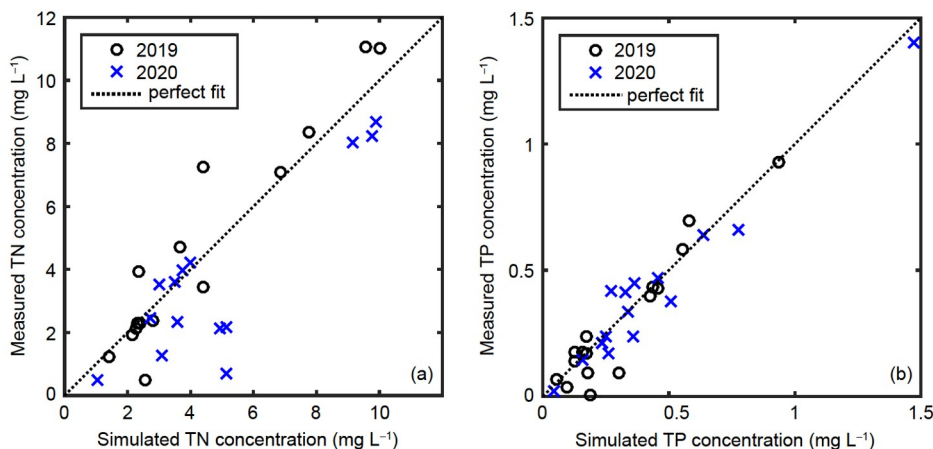


Figure 6 Comparison of the measured and simulated TN (a) and TP (b) concentrations in typical water bodies.

0.95, respectively, while bias values of 68.8% and 56.3% for total water bodies are excellent (± 0.20 or less) and those of 93.8% and 62.5% for total water bodies are good (± 0.40 or less), respectively; the correlation coefficients of TP concentration are 0.95 and 0.97, and bias values of 62.5% and 62.5% for total water bodies are excellent and those of 75.0% and 81.3% for total water bodies are good, respectively. Moreover, the export coefficients of nonpoint source TN and TP at all hydrological response units are 1.8–1.9 $\text{t km}^{-2} \text{yr}^{-1}$ and 0.15–0.19 $\text{t km}^{-2} \text{yr}^{-1}$, respectively (for comparison, 2.7 $\text{t km}^{-2} \text{yr}^{-1}$ and 0.15–0.30 $\text{t km}^{-2} \text{yr}^{-1}$ estimated by Wuhan Ecological Environmental Condition Bulletin 2020 and Qin (2020), respectively); the TN export coefficient is about 30% lower, whereas the TP export coefficient is in good agreement.

The statistical values of the 18 indicators related to socioeconomic development, infrastructure development, and social water cycle during 2001–2012 and 2013–2020 are employed for calibration and validation of the socioeconomic development and its water cycle module (Figure 7). Bias, correlation coefficients, and NSEs of 100%, 83.3%, and 69.4% of the indicators are in the excellent class (i.e., bias within ± 0.30 , correlation coefficient > 0.80 , and NSE > 0.65). The simulation performance of socioeconomic indicators is the best among all indicators, all of which are in the excellent class, especially urban population, tertiary GDP, and total GDP, followed by the infrastructure development and social water cycle indicators, particularly road area, sewage length, water consumption per 10^4 yuan GDP, and domestic water consumption. However, the simulation performance of the industrial water consumption in the validation period is a little worse, mainly due to the large interannual fluctuations in the industrial water consumption.

4.4 Urban water system assessment and regulation

Flooding in the PPP zone is simulated under the design

rainfall conditions for return periods of 10 and 50 yr with/without the source LID control. The results present a relatively high flood risk in the area with the current land surface and drainage network system, where flood depths in some areas reached or exceeded the threshold value for the high flood risk area (> 0.4 m); this is mainly because these areas are low-lying or have large impervious surface areas. LID measures, such as grass swales, recessed green spaces, and permeable pavement, can reduce the maximum inundated area by 32.6% and 22.5% under the design rainfall conditions for the 10-year and 50-year return periods, respectively. Therefore, the LID measures considerably mitigate urban waterlogging by reducing surface impermeability and retaining rainwater. However, this performance gradually reduces with increasing rainfall return period. Zhou et al. (2022) presented detailed information.

Based on the simulation and evaluation results of the black and odorous levels in Wuhan in 2020 (Figure 8a), the area with black and odorous water corresponds to 84.4 km^2 , accounting for 13.3% of the total urban water area. The simulation results are consistent with the measured assessment results in 90.5% of the water bodies. No black and odorous water is present along the Yangtze River and in the downtown area, except for a small amount of black and odorous water around the Wuhu Lake and Dongshan Street, which is mainly due to the internal source release from sediment and suburban nonpoint source pollution. The three treatment process combinations (i.e., the ecological restoration, active water circulation, and artificial enhancement) could be mainly realized with the nitrogen and phosphorus removal and dissolved oxygen increase through biochemical and oxidation reactions, which then enhance the removal ratio of the black and odorous water. The average removal ratios of the three process types are approximately 45%, 42%, and 65%, respectively (Figure 8b–8d). Additionally, the costs of all the processes range from 62 to 426 million yuan. Among them, the average costs of ecological restoration, active

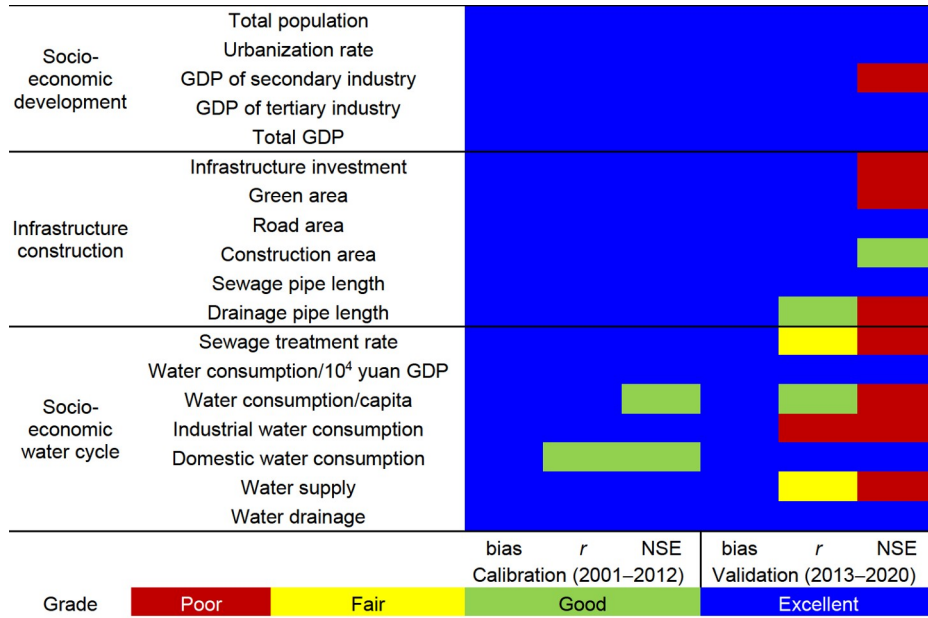


Figure 7 Simulation performance of the key indicators of the socioeconomic development and its water cycle submodule.

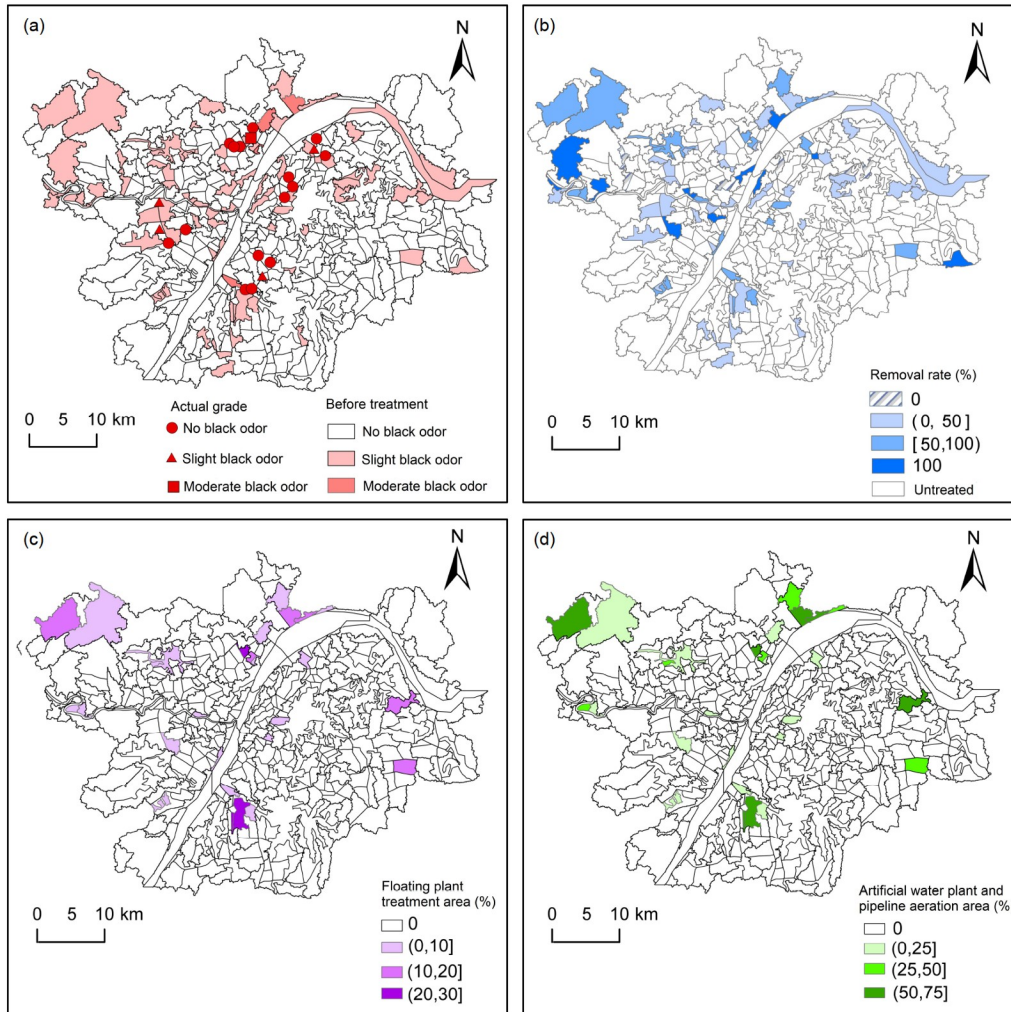


Figure 8 Spatial distribution of the assessment and treatment measures for black and odorous water in Wuhan in 2020.

water circulation, and artificially enhanced treatment are 271, 82, and 189 million yuan, respectively.

From the simulation and evaluation results of the eutrophication level in Donghu Lake in 2020, the water areas of mild and moderate eutrophication levels are observed to account for 91% and 5% of the total lake area, respectively (Figure 9a), in good agreement with the evaluation results from Wuhan City Water Resources Bulletin 2020. The primary causes of eutrophication are excessive inputs of pollutant loads and internal release of nutrients from lake

sediments. The costs and performance of multilevel ecological restoration measures in the library provided by the UWS5.0 model are evaluated, and the results reveal that a combination of source reduction (vegetated ditches), pathway interception (riparian wetlands), and terminal treatment (submerged plants, ecological floating islands, and emergent plants) approaches could realize the most cost-effective outcome (Figure 9c–9e), and the cumulative reduction of the eutrophication level in the comprehensive nutrient status index is 37% (Figure 9b). The source reduction, pathway

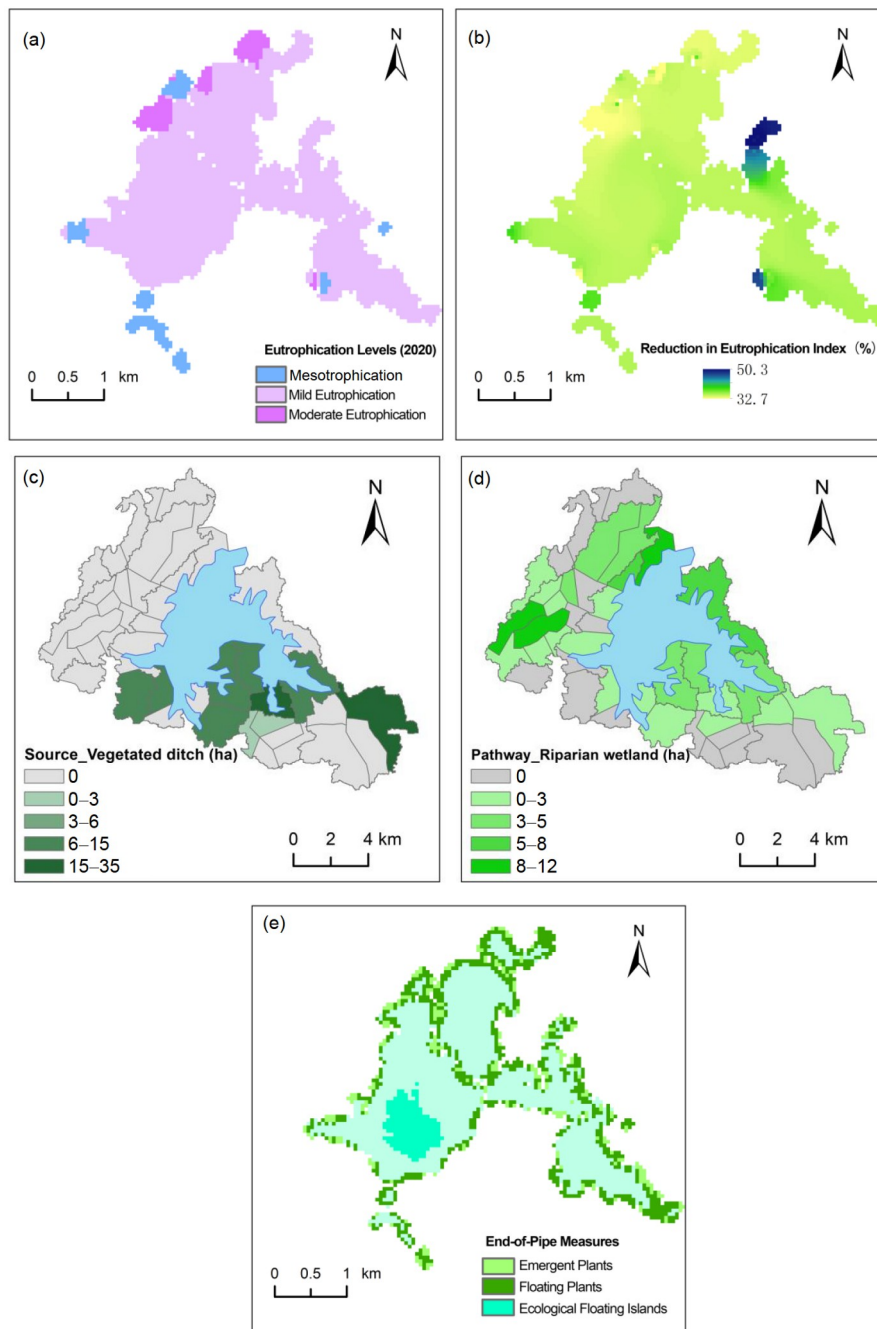


Figure 9 Spatial distribution of the eutrophication assessment and treatment measures in Donghu Lake in 2020.

interception, and terminal treatment reduced pollutant loads and comprehensive nutrient status index by decreasing the nonpoint source accumulation-flushing intensity, pollution load of the lake inflow, and internal nutrient release. The reduction rates in the comprehensive nutrient status index for the three measure types are 1%, 25%, and 15%, with corresponding costs of 0.2×10^8 , 10.5×10^8 , and 3.7×10^8 yuan, respectively.

Based on the simulation and evaluation by the UWS 5.0 model, the green development index under the current conditions in 2020 in Wuhan City is 0.56 (Figure 10), and the contributions of the five dimensions, namely, resource utilization, environmental quality, ecological protection, economic growth, and green life, are 13.8%, 31.5%, 3.2%, 27.7%, and 23.8%, respectively. The ecological protection dimension is the main constraint to green development. With the implementation of the abovementioned improved measures of waterlogging, black and odorous water bodies, and lake eutrophication, the green development index increases remarkably to 0.67, with an increase of 21%. The contributions of the five dimensions are 11.1%, 32.2%, 15.4%, 22.2%, and 19.1%, respectively, with the ecological protection dimension index improving the most remarkably.

5. Conclusions

In this paper, the concept, theoretical foundations, key technologies, and theoretical development of the urban water

system are described. The UWS 5.0 model is developed using the TVGM_Urban rainfall-runoff model as the core and integrating the natural-social water cycle and its associated water environmental, water ecological, and human processes with the effect of multiscale sponge measures. The model is validated in Wuhan City in the Yangtze River Economic Belt. The following conclusions can be drawn from this study.

(1) A complete urban water system should consider the city and its associated rivers, lakes, and wetlands as the research object and explore the integration mechanisms of the “rainfall-evapotranspiration-storage-runoff” natural water cycle, “supply-use-consumption-discharge” artificial water cycle, and river regulation inside and outside the city, as well as regulation mechanism of socioeconomic development and sponge measures on water quantity-quality-ecological processes. Its theoretical basis includes the urban water cycle theory, biogeochemical cycle theory, water ecosystem health theory, urban economic theory, and sustainable development theory.

(2) The UWS 5.0 model achieved five main simulation functions, including rainfall-runoff-nonpoint source pollutant load, water and pollutant transportations through the drainage network system, terminal regulation and purification, socioeconomic water cycle, and water system assessment and regulation. The model performs well for simulations of the rainfall-runoff process, pollutant concentration in the water body, and characteristic indicators of the socioeconomic development in Wuhan City. When the

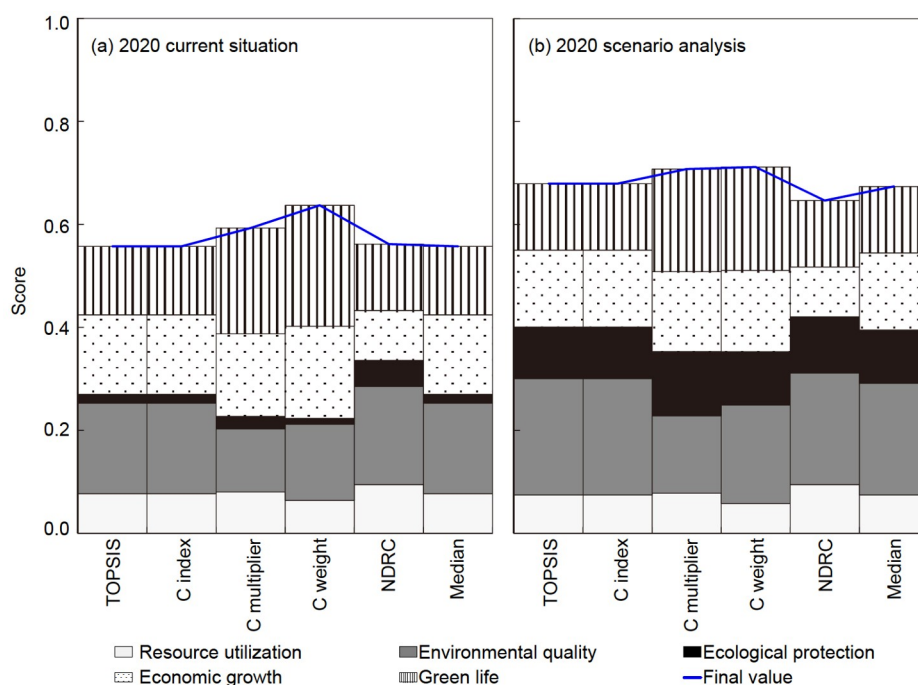


Figure 10 Green development level and regulation performance in 2020. C index, C multiplier, and C weight represent the comprehensive index, comprehensive multiplier, and comprehensive weight methods, respectively. NDRC denotes the NDRC evaluation method, while the median is the median value of the five evaluation methods.

measured and simulated processes are compared, the correlation coefficients and NSEs of all the rainfall-runoff events are found to be in excellent and good classes, respectively. The bias values of the simulated TN and TP concentrations are in good class in the case of 78.1% of the 16 investigated water bodies, and their corresponding correlation coefficients are 0.96 and 0.92, respectively. The simulation of 18 socioeconomic indicators provide excellent bias, correlation coefficient, and NSE values of 100%, 83.3%, and 69.4% to total indicators, respectively.

(3) According to the simulation and evaluation of waterlogging points, black and odorous level of water bodies, lake eutrophication level, and green development level and their spatial distributions in Wuhan City, the sponge, artificial enhancement, and source reduction-path interception-terminal treatment pathway measures are proposed to mitigate waterlogging, black and odorous water bodies, and lake eutrophication, respectively. The maximum inundated area for a once-in-10-years rainfall event is reduced by 32.6%, the removal rate of the black and odorous water bodies is 65%, and the comprehensive trophic state index of the water bodies is reduced by 37%. As a consequence, the green development level in Wuhan City in 2020 increased from 0.56 to 0.67, which is the most significant increase with respect to the ecological protection dimension.

This study primarily investigates the theory and modeling of urban water systems, which, to some extent, advance the integration of various disciplines associated with cities and water. Future work should be done to further improve the conceptual and theoretical-technical system of urban water systems, optimize the model structure and extend the model functions, strengthen the observation of water system-related processes and collection of basic information to support validation of model simulation performance, and improve the effectiveness of the UWS 5.0 model to solve complex urban water issues.

Acknowledgements This research was supported by the Strategic Priority Research Program of the Chinese Academy of Sciences (Grant No. XDA23040301) and the National Natural Science Foundation of China (Grant No. 42071041).

Conflict of interest The authors declare that they have no conflict of interest.

References

Amaguchi H, Kawamura A, Olsson J, Takasaki T. 2012. Development and testing of a distributed urban storm runoff event model with a vector-based catchment delineation. *J Hydrol*, 508: 240–253

Balchin P N, Isaac D, Chen J. 2000. *Urban Economics—A Global Perspective*. Basingstoke: Palgrave Macmillan. 560

Bauer P, Dueben P D, Hoefler T, Quintino T, Schulthess T C, Wedi N P. 2021. The digital revolution of Earth-system science. *Nat Comput Sci*, 1: 104–113

Beal L, Senison J, Banner J, Musgrove M L, Yazbek L, Bendik N, Her-

ington C, Reyes D. 2020. Stream and spring water evolution in a rapidly urbanizing watershed, Austin, TX. *Water Resour Res*, 56: e2019WR025623

Bhaduri A, Bogardi J, Leentvaar J, Marx S. 2014. *The Global Water System in the Anthropocene: Challenges for Science and Governance*. Bonn: Springer International Publishing. 437

Chambers L G, Chin Y P, Filippelli G M, Gardner C B, Herndon E M, Long D T, Lyons W B, Macpherson G L, McElmurry S P, McLean C E, Moore J, Moyer R P, Neumann K, Nezat C A, Soderberg K, Teutsch N, Widom E. 2016. Developing the scientific framework for urban geochemistry. *Appl Geochem*, 67: 1–20

Chen J N, Dong X. 2007. Developments and challenges in urban water system planning (in Chinese). *Water Wastewater Eng*, 33: 1–16

Chen J X, Zhang J H, Peng J B, Zou L, Fan Y J, Yang F R, Hu Z W. 2023. Alp-valley and elevation effects on the reference evapotranspiration and the dominant climate controls in Red River Basin, China: Insights from geographical differentiation. *J Hydrol*, 620: 129397

Chen X. 2018. Study on the impacts of underlying surface change on the waterlogging in the downtown area of Wuhan (in Chinese). Dissertation for Master's Degree. Wuhan: Wuhan University

Cheng G D, Li X. 2015. Integrated research methods in watershed science. *Sci China Earth Sci*, 58: 1159–1168

Dong X, Yang K Z. 2021. Urban economics research in China: Review of the 13th five year plan period and prospect of the 14th five year plan period (in Chinese). *Urban Develop Stud*, 28: 63–69

Dou M, Song S J, Shi Y X, Jin M. 2022. Two-stage optimization of urban water system connectivity scheme under structure-function coupling (in Chinese). *Adv Water Sci*, 33: 79–90

Fang C L, Bao C, Shen Y M. 2004. Analysis on the characteristic and the change trend of urban expansion restricted by water resources in the arid area of Northwest China—A case study of the cities in the Western Long Hai-Lan Xin Economic Zone (in Chinese). *J Nat Resour*, 19: 248–256

Fang C L, Zhou C H, Gu C L, Chen L D, Li S C. 2016. Theoretical analysis of interactive coupled effects between urbanization and eco-environment in mega-urban agglomerations (in Chinese). *Acta Geogr Sin*, 71: 531–550

Freni G, Mannina G, Viviani G. 2008. Uncertainty in urban stormwater quality modelling: The effect of acceptability threshold in the GLUE methodology. *Water Res*, 42: 2061–2072

Fu C, Li Y X, Wang S T. 2017. Analysis of water system structure and connectivity in the center of Nanchang under the urbanization process (in Chinese). *Resour Environ Yangtze Basin*, 26: 1042–1048

Gu C L, Duan X J, Yu T F, Sun Y Z, Chen Q N. 2002. A study on the key techniques of the digital city and its 3D re-appearing (in Chinese). *Geogr Res*, 21: 14–24

GWSP. 2005. *The Global Water System Project: Science Framework and Implementation Activities*. Earth System Science Partnership. Technical Report. Global Water System Project Office, Bonn, Germany. 78

Hu C, Xia J, She D, Song Z, Zhang Y, Hong S. 2021. A new urban hydrological model considering various land covers for flood simulation. *J Hydrol*, 603: 126833

Hu Q F, Zhang J Y, Wang Y T, Huang Y, Liu Y, Li L J. 2018. A review of urbanization impact on precipitation (in Chinese). *Adv Water Sci*, 29: 138–150

Jiang E H, Wang Y J, Tian S M, Li J H, Xu L J, Zhang X P. 2020. Exploration of watershed system science (in Chinese). *J Hydraul Eng* 51: 1026–1037

Karr J R, Fausch K D, Angermeier P L, Yant P R, Schlosser I J. 1986. *Assessing Biological Integrity in Running Waters: A Method and Its Rationale*. Illinois: Illinois Natural History Survey

Liang H, Pan X F, Yu X F, Xu W, Chen H M, Li X K. 2016. Valuation of water ecosystem services in Shenzhen city (in Chinese). *J Nat Resour*, 31: 1474–1487

Liu C M, Zhang Y Y, Wang Z G, Wang Y L, Bai P. 2016. The LID pattern for maintaining virtuous water cycle in urbanized area: A preliminary study of planning and techniques for sponge city (in Chinese). *J Nat*

- Resour, 31: 719–731
- Liu D. 2009. Impact of urbanisation on rain-flood runoff—a case study of Wuhan city (in Chinese). *J Entrepreneurship Sci Technol*, 22: 66–67, 71
- Liu J G, Hull V, Godfray H C J, Tilman D, Gleick P, Hoff H, Pahl-Wostl C, Xu Z C, Chung M G, Sun J, Li S X. 2018. Nexus approaches to global sustainable development. *Nat Sustain*, 1: 466–476
- Liu J H, Wang H, Gao X R, Chen S L, Wang J L, Shao W W. 2014. Review on urban hydrology (in Chinese). *Chin Sci Bull*, 59: 3581–3590
- Lu Z X, Wei Y, Feng Q, Xiao H L, Chen G D. 2016. Progress on socio-hydrology (in Chinese). *Adv Water Sci*, 27: 772–783
- Moriasi D N, Arnold J G, Van L M W, Binger R L, Harmel R D, Veith T. 2007. Model evaluation guidelines for systematic quantification of accuracy in watershed simulations. *Trans ASABE*, 50: 885–900
- Neitsch S, Arnold J, Kiniry J, Williams J R. 2011. SWAT2009 Theoretical Documentation. Texas: Texas Water Resources Institute
- Obropta C C, Kardos J S. 2007. Review of urban stormwater quality models: Deterministic, stochastic, and hybrid approaches. *J Am Water Resour Assoc*, 43: 1508–1523
- Qin L, Zhu J L, Gong H Q, Wang M, Chen M. 2020. Analysis of pollution source and calculation of pollution load of the South Lake (in Chinese). *J Hubei Univ-Nat Sci*, 42: 298–305
- Ren N Q, Feng Y J, Chen Z L, Chen W, Zhang Z H. 2012. Transformation Rules of Pollutants in Urban Water Systems and Resource Utilization Theory and Technology (in Chinese). Beijing: Science Press
- Ren Y F, Wang X K, Han B, Ouyang Z Y, Miao H. 2005. Chemical analysis on stormwater-runoff pollution of different underlying urban surfaces (in Chinese). *Acta Ecol Sin*, 25: 3225–3230
- Ritter A, Muñoz-Carpena R. 2013. Performance evaluation of hydrological models: Statistical significance for reducing subjectivity in goodness-of-fit assessments. *J Hydrol*, 480: 33–45
- Santhi C, Arnold J G, Williams J R, Dugas W A, Srinivasan R, Hauck L M. 2001. Validation of the SWAT model on a large river basin with point and nonpoint sources. *J Am Water Resour Assoc*, 37: 1169–1188
- Shao Y S. 2004. Control and plan of city water system (in Chinese). *City Plann Rev*, 10: 62–67
- Shen W J, Shen Z R, Wang X Y. 2004. Ecosystem health theory and its analysis method (in Chinese). *Chin J Eco-Agricul*, 12: 159–161
- Shepherd J M, Pierce H, Negri A J. 2002. Rainfall modification by major urban areas: Observations from spaceborne rain radar on the TRMM satellite. *J Appl Meteorol*, 41: 689–701
- Sina M, Anik B. 2013. Understanding the global water system for water cooperation. In: Griffiths J, Lambert R, eds. *Free Flow, Reaching Water Security through Cooperation*. Paris: UNESCO Publishing and Tudor Rose. 288–290
- Sivapalan M, Savenije H H G, Blöschl G. 2012. Socio-hydrology: A new science of people and water. *Hydrol Process*, 26: 1270–1276
- Smith J A, Baeck M L, Morrison J E, Sturdevant-Rees P, Turner-Gillespie D F, Bates P D. 2002. The regional hydrology of extreme floods in an urbanizing drainage basin. *J Hydrometeorol*, 3: 267–282
- Sui J, Wang H L, Li J. 2016. Development and application of water quality model for urban drainage system (in Chinese). *China Water Wastewater*, 32: 130–134
- Tang Q H. 2020. Global change hydrology: Terrestrial water cycle and global change. *Sci China Earth Sci*, 63: 459–462
- Tian F Q, Cheng T, Lu Y, Xu Z X. 2018. A review on socio-hydrology and urban hydrology (in Chinese). *Prog Geogr*, 37: 46–56
- Wang H, Wang J, Liu J H, Mei C. 2021. Analysis of urban water cycle evolution and countermeasures (in Chinese). *J Hydraul Eng* 52: 3–11
- Wang M C, Liu X Q, Zhang J H. 2002. Evaluate method and classification standard on lake eutrophication (in Chinese). *Environ Monitor China*, 18: 47–49
- Wang X, Wang Y G, Sun C H, Pan T. 2016. Formation mechanism and assessment method for urban black and odorous water body: A review (in Chinese). *Chin J Appl Ecol*, 27: 1331–1340
- Wang Y L, Liang Q H, Kesserwani G, Hall J W. 2011. A 2D shallow flow model for practical dam-break simulations. *J Hydraulic Res*, 49: 307–316
- Xia J. 2023. Toward water systems science and technology, in the section of the frontiers of water and sanitation. *Nature Water*, 1: 10–18
- Xia J, Wang G S, Tan G, Ye A Z, Huang G H. 2005. Development of distributed time-variant gain model for nonlinear hydrological systems. *Sci China Ser D-Earth Sci*, 48: 713–723
- Xia J, Zhang Y Y, Mu X M, Zuo Q T, Zhou Y J, Zhao G J. 2021. A review of the ecohydrology discipline: Progress, challenges, and future directions in China. *J Geogr Sci*, 31: 1085–1101
- Xia J, Zhang Y Y, Xiong L H, He S, Wang L F, Yu Z B. 2017. Opportunities and challenges of the sponge city construction related to urban water issues in China. *Sci China Earth Sci*, 60: 652–658
- Xia J, Zhang Y Y, Wang Z G, Li H. 2006. Water carrying capacity of urbanized area (in Chinese). *J Hydraul Eng*, 37: 1482–1488
- Xu G L, Xu Y P, Xu H L. 2010. Advance in hydrologic process response to urbanization (in Chinese). *J Nat Resour*, 25: 2171–2178
- Xu W J, Cao S L. 2009. Calculation method of eco-environmental water demand of urban lake with an example of Dongchang Lake in Liaocheng City of China (in Chinese). *J Hydroel Eng*, 28: 102–107
- Xu Z X, Cheng T. 2019. Basic theory for urban water management and sponge city—review on urban hydrology (in Chinese). *J Hydraul Eng*, 50: 53–61
- Xu Z X, Zhou C F, Pan P, Li J F, Xie C. 2020. Influences of urban lakes eutrophication on the C, N and P stoichiometric characteristics in leaves of aquatic macrophytes (in Chinese). *Resour Environ Yangtze Basin*, 29: 1324–1332
- Yan Y T, Jiang Y Z, Liang L L, Zhao H L, Gu J J, Dong J P, Cao Y, Duan H. 2022. Digital twin watershed: new infrastructure and new paradigm of future watershed governance and management (in Chinese). *Adv Water Sci*, 33: 683–704
- Yang Y, Liu Y, Jin F J, Dong W, Li L. 2012. Spatio-temporal analysis of urbanization and land and water resources efficiency of oasis cities in tarim riverbasin (in Chinese). *Acta Geogr Sin*, 67: 157–168
- Yang Z F, Cheng H G. 2002. Models in simulation system of urban industrial water pollution control (in Chinese). *Acta Sci Circum*, 22: 213–218
- Ye Y T, Jiang Y Z, Liang L L, Zhao H L, Gu J J, Dong J P, Cao Y, Duan H. 2022. Digital twin watershed: new infrastructure and new paradigm of future watershed governance and management (in Chinese). *Adv Water Sci*, 27: 683–704
- Yu H X, Xu L Q, Chen X H, Zhang Q. 2011. Regulation mechanism and evaluation model of urban water ecosystem (in Chinese). *J Nat Resour*, 26: 1707–1714
- Zhang J Y, Song X M, Wang G Q, He R M, Wang X J. 2014. Development and challenges of urban hydrology in a changing environment: Hydrological response to urbanization (in Chinese). *Adv Water Sci*, 25: 594–605
- Zhang J, Li D. 2010. Theory and strategy on healthy circulation of urban water system (in Chinese). *J Harbin Inst Technol*, 42: 849–854, 868
- Zhang X F, Liu Z W, Xie Y F, Chen G R. 2007. Evaluation on the changes of ecosystem service of urban lakes during the degradation process: a case study of Xiannv Lake in Zhaoqing, Guangdong Province (in Chinese). *Acta Ecol Sin*, 27: 2349–2354
- Zhang Y Y, Hou J J, Xia J, She D X, Wu S J, Pan X Y. 2022. Regulation characteristics of underlying surface on runoff regime metrics and their spatial differences in typical urban communities across China. *Sci China Earth Sci*, 65: 1415–1430
- Zhang Y Y, Pang X, Xia J, Shao Q X, Yu E T, Zhao T T G, She D X, Sun J Q, Yu J J, Pan X Y, Zhai X Y. 2019. Regional patterns of extreme precipitation and urban signatures in metropolitan areas. *J Geophys Res-Atmos*, 124: 641–663
- Zhang Y Y, Shao Q X, Taylor J A. 2016a. A balanced calibration of water quantity and quality by multi-objective optimization for integrated water system model. *J Hydrol*, 538: 802–816
- Zhang Y Y, Shao Q X, Ye A Z, Xing H T, Xia J. 2016b. Integrated water system simulation by considering hydrological and biogeochemical processes: model development, with parameter sensitivity and auto-calibration. *Hydrol Earth Syst Sci*, 20: 529–553

- Zhang Y Y, Shao Q X. 2018. Uncertainty and its propagation estimation for an integrated water system model: An experiment from water quantity to quality simulations. *J Hydrol*, 565: 623–635
- Zhang Y Y, Xia J, Wang Z G. 2007. Research on regional water resources carrying capacity theory and method (in Chinese). *Progr Geogr*, 26: 12–132
- Zhang Y Y, Xia J, Yu J J, Randall M, Zhang Y C, Zhao T T G, Pan X Y, Zhai X Y, Shao Q X. 2018. Simulation and assessment of urbanization impacts on runoff metrics: Insights from landuse changes. *J Hydrol*, 560: 247–258
- Zhao Y W, Yang Z F. 2005. Preliminary study on assessment of urban river ecosystem health (in Chinese). *Adv Water Sci*, 16: 349–355
- Zhou K, Chen Y F, Xu Y. 2022. Associated effects and interaction mechanism of urban expansion and water pollutant emissions: A case study of the Yangtze River delta from 2011 to 2015 (in Chinese). *Acta Ecol Sin*, 42: 3167–3180
- Zhou Y, She D X, Wang Y L, Xia J, Zhang Y Y. 2022. Evaluating the impact of low impact development practices on the urban flooding over a humid region of China. *J Am Water Resour Assoc*, 58: 1264–1278
- Zou L, Liu H Y, Wang F Y, Chen T, Dong Y. 2022. Regional difference and influencing factors of the green development level in the urban agglomeration in the middle reaches of the Yangtze River. *Sci China Earth Sci*, 65: 1449–1462
- Zuo Q T, Ma J X, Gao C C. 2005. Study on carrying capacity of urban water environment (in Chinese). *Adv Water Sci*, 16: 103–108

(Editorial handling: Xiaoyan LI)